KALIRIN: NOVEL ROLE IN OSTEOCYTE FUNCTION

Kornchanok Wayakanon, DDS

Submitted to the Graduate Faculty of the School of Dentistry in fulfillment of the requirement for the

Degree of Master of Science in Dentistry

Indiana University School of Dentistry, November 2013

This thesis accepted by the faculties of the Department of Operative Dentistry in the Indiana University School of Dentistry in partial fulfillment of the requirements for the Degree of Master of Science in Dentistry.

_____

Dr. Lester Jack Windsor

_____

Dr. Tien-Min Gabriel Chu

_____

Dr. Sopanis Cho

_____

Dr. Angela Bruzzaniti
Chair of the Research Committee

_____

Dr. Norman Blaine Cook
Program Director

Date

ACKNOWLEDGEMENTS

There are many people whom I would like to thank for their contribution and support. This research study and thesis would not be possible without them.

I would like to thank all those involved at Naresuan University and the Royal Thai Government who have made the undertaking of this MSD possible through their valuable financial support.

A huge gratitude is given to my supervisor, Dr. Angela Bruzzaniti, for an exceptional idea for this research project, her scientific advice and guidance, and for her encouragement and patience, particularly in reading and correcting the drafts of my proposal and thesis.

I would like to thank Dr. Su Huang for his suggestions and guidance in PCR, QPCR, and Western Blot Assays. Thanks to Dr. Pierre Eleniste for his suggestions regarding immunofluorescent staining and animal experiments. Thanks to Dr. Matthew Allen Department of Anatomy and Cell Biology, and the Histology Department, School of Medicine for basic fuchsin osteocyte staining. I wish to thank Dr. Lilian Plotkin, Department of Anatomy and Cell Biology, and the members Microscopy Center, School of Medicine for bone acid-etching preparations and SEM analyses. Thanks also go to Mr. George Eckert for statistical consultations, Ms. Anissa Mahmoudi for mice genotyping and Mr. Ajaydeep Singh for laboratory assistance.

I would like to thank Ms. Karen Wilczewski and Dr. Wai Ching Liu for proofreading and grammatical editing this thesis. I really appreciate their help.

I am grateful to Dr. Norman Blaine Cook, the program director, for giving me the opportunity to study in the Graduate Operative program and supervising me throughout the postgraduate program. I would like to thank all of the committee members: Dr. Lester Jack Windsor, Dr. Tien-Min Gabriel Chu, and Dr. Sopanis Cho for their valuable time and advice.

Most importantly, I would like to express my gratitude to my family, especially my parents and brothers, for their moral support and molecular biology consultations.

TABLE OF CONTENTS

TABLE OF CONTENTS

Page

INTRODUCTION…… 1

OBJECTIVES …….. 3

HYPOTHESES……. 3

REVIEW OF LITERATURE……... 4

MATERIALS AND METHODS…….. 12

RESULTS……. 21

TABLES……... 28

FIGURES…….. 34

DISCUSSION……... 54

SUMMARY AND CONCLUSIONS……... 60

REFERENCES……. 62

ABSTRACT…….. 74

CURRICULUM VITAE……... 76

LIST OF TABLES

LIST OF TABLES

TABLE 1. Osteoblast signaling and regulatory proteins…….. 29

TABLE 2. Osteocyte signaling and regulatory proteins…….. 30

TABLE 3. Antibodies for Western blotting and immunofluorescent staining……. 31

TABLE 4. Oligonucleotide primers used for QPCR…….. 32

TABLE 5. Analyses of osteocyte cytoplasmic processes from Kal-KO and WT mice…… 33

LIST OF FIGURES

LIST OF FIGURES

Figure 1. Schema for mesenchymal stem cell differentiation into osteoblasts……...…… 35

Figure 2. Schema describing the osteocyte differentiation process ……..... 36

Figure 3. Signaling between bone cells……...… 37

Figure 4. The domain structure of Kalirin isoforms……..…… 38

Figure 5. Mice tibias and femurs before and after bone marrow removal…….. 39

Figure 6. Domain structure of the Kalirin cDNA expression constructs……..... 40

Figure 7. Determination of Kalirin mRNA and proteins levels in osteocytes……...…. 41

Figure 8. Immunofluorescent labeling of Kalirin in primary osteoblasts……..……. 42

Figure 9. Immunofluorescent labeling of Kalirin in WT osteocytes……...……... 43

Figure 10. Immunofluorescent labeling of Kalirin in MLO-Y4 cells……...… 44

Figure 11. Basic fuchsin staining of osteocytes in cortical bone……..... 45

Figure 12. Analyses of osteocytes from Kal-KO and WT mice by SEM……..... 46

Figure 13. The morphology of primary osteocytes from WT and Kal-KO mice…….…..... 47

Figure 14. Comparison of mRNA expression levels in WT and Kal-KO osteocytes……..…..… 48

Figure 15. The morphology of MLO-Y4 cells after treatment with NGF or KCl……...…. 49

Figure 16. Western blot analyses of MLO-Y4 cells treated with NGF or KCl……..... 50

Figure 17. Western blot analyses of MLO-Y4 cells expressing the Kalirin-12 kinase domain……..... 51

Figure 18. Immunofluorescent labeling of MLO-Y4 cells expressing the Kalirin-12 kinase domain..... 52

Figure 19. Working model for the mechanisms of action of Kalirin in osteocytes…….. 53

ABBREVIATIONS

ABBREVIATIONS

α-MEM	α-Minimum Essential Medium
aa	Amino acid
BCS	Bovine calf serum
BMD	Bone mineral density
BSA	Bovine serum albumin
cDNA	Complementary DNA
CDUs	Collagenase digestive units
Ct	Threshold cycle
CZH	CDM and Zizimin homology
DH	Dbl-homology
ECL	Enhanced chemiluminescence
FBS	Fetal bovine serum
GDP	Guanosine diphosphate
GEF	Guanine nucleotide exchange factor
GFP	Green fluorescent protein
GTP	Guanosine triphosphate
Ig-FNIII	Immunoglobulin-fibronectin III
Kal-KO	Kalirin-knockout
KCl	Potassium chloride
LB	Luria-Bertani
LRP	Lipoprotein receptor-related proteins
M-CSF	Macrophage colony-stimulating factor
MLO-Y4	Murine long bone osteocyte Y4
MMA	Methyl methacrylate
MT1-MMP	Membrane-type matrix metalloproteinase-1
NGF	Nerve growth factor

OPG	Osteoprotegerin
PBS	Phosphate buffer saline
PCR	Polymerase chain reaction
pERK	Phosphorylated extracellular-signal-regulated kinase
PGE2	Prostaglandin E_2
PH	Pleckstrin-homology
QPCR	Quantitative real-time PCR
RANKL	Receptor activator of nuclear factor kappa-B ligand
S.O.C	Super optimal broth with catabolite repression
Ser-Thr	Serine-threonine
TE	Tris-EDTA
tERK	Total extracellular-signal-regulated kinase
TNF	Tumor necrosis factor
WT	Wild-type

INTRODUCTION

Osteoporosis is a skeletal disorder characterized by low bone mineral density (BMD) and deterioration of the bone architecture which compromises bone strength, predisposing it to an increase in the risk of fractures. The occurrence of osteoporosis increases as the population age increases, and is especially common in post-menopausal women. There are approximately 200 million people around the world who suffer from osteoporosis. It is anticipated that one-third of women and one-fifth of men over 50-years of age will experience an osteoporotic fracture in their lifetime[1].

Bone remodeling is a lifelong process. Mature bone is removed by a process of bone resorption by osteoclasts and new bone is formed by osteoblasts. The bone remodeling cycle controls the replacement of bone following injury, including large bone fractures and smaller micro-fractures. The remodeling process is regulated by balancing the bone formation and bone resorption processes. When the balance between bone formation and bone resorption is disrupted, a decrease in bone mineral density leading to osteoporosis can ensue. Osteocytes are another important bone cell type. Osteocytes are fully differentiated osteoblasts embedded in mineralized bone lacuna. They play a vital role in cellular communication and regulate the functions of both osteoblasts and osteoclasts. They are in direct communication with each other and with the other bone cell types through cytoplasmic membrane extensions known as dendritic spines, which travel through canaliculi within the bone matrix.

Kalirin is a novel guanine nucleotide exchange factor (GEF) originally identified in the brain. Several studies have reported that Kalirin is involved in the formation of the dendritic spines of neurons and intercellular synapses. Recent studies conducted in Dr. Bruzzaniti's laboratory demonstrated that Kalirin is expressed in osteoblasts and osteoclasts. Female Kalirin-knockout (Kal-KO) mice exhibited 45% lower bone volume compared with wild type (WT) mice at 14 weeks of age, while Kal-KO male mice exhibited 19% lower bone volume than control male mice. In addition, a reduction in cortical area was found in Kal-KO female mice. These studies revealed that female Kal-KO mice are osteoporotic.

Based on several findings, it was hypothesized that Kalirin may regulate the morphology and function of osteocytes; i) Kalirin is expressed in osteoblasts and osteoclasts, ii) Kalirin plays a role in regulating bone

mass, and iii) Kalirin regulates the cytoskeleton of neuronal cells. In the current study, the expression of Kalirin isoforms was examined in primary osteocytes and in the osteocytic cell line, MLO-Y4. The morphology of primary osteocytes from WT and Kal-KO mice were compared by microscopy and the expression level of important signaling proteins in osteocytes were determined by quantitative real-time PCR (QPCR). In addition, the effects of Kalirin expression on the formation of cytoplasmic processes in MLO-Y4 cells were examined. Findings from this study provide insights into the role of Kalirin in osteocytes and its mechanisms of action in the regulation of bone mass.

OBJECTIVES

1. To determine the role of Kalirin in the regulation of osteocyte morphology and functions.
2. To determine the expression of Kalirin in primary osteocytes and MLO-Y4 osteocytic cells.

HYPOTHESES

1. Osteocytes derived from WT mice will exhibit longer cytoplasmic processes and will exhibit differences in cellular functions compared with osteocytes from Kal-KO mice.
2. Overexpression of Kalirin in MLO-Y4 cells will lead to elongation of cytoplasmic processes and affect osteocyte functions.

REVIEW OF LITERATURE

Bone modeling occurs during skeletal growth to increase the size of bones and alter their shape. Bone modeling occurs on the periosteal surface without prior bone resorption[2]. The deposition of osseous tissue at the periosteal surface increases the stiffness of bone, resulting in rapid strengthening of the cylindrical-shaped bone. There are two types of bone formation processes: endochondral ossification and intramembranous ossification. During endochondral ossification, the cartilage scaffold is replaced by bone whereas during intramembranous ossification, bone formation occurs without an intermediate cartilage step[3]. Unlike bone modeling, bone remodeling is a surface-dependent process that does not lead to alteration of the size and shape of bone. It occurs on endocortical, intracortical and trabecular regions of the bone. The bone remodeling process starts with bone resorption by osteoclasts and takes 2-3 weeks and is then followed by a period of bone formation by osteoblasts, which occurs over 2-3 months[4].

Bone remodeling is regulated by three bone cell types; osteoclasts, osteoblasts and osteocytes. An equilibrium between bone formation and bone resorption is regulated by the coordinated activities of osteoclasts, osteoblasts and osteocytes[5,6]. An imbalance between osteoclast and/or osteoblast functions can lead to bone loss and osteoporosis. Osteoporosis is a skeletal disorder characterized by porous, thin and weak bones that become fragile and break easily. It occurs especially in women following menopause. Osteoporosis causes 8.9 million fractures annually worldwide, most commonly occurring in the wrist, hip, and vertebrae [7]. Osteoporosis medicaments are classified into 2 groups: anti-resorptives and anabolic drugs. Bisphosphonates, calcitonin, estrogen, and selective estrogen receptor modulators (SERMs) and Denosumab, an antibody to receptor activator of the nuclear factor kappa-B ligand (RANKL), are examples of anti-resorptive or anti-catabolic drugs. Bisphosphonates and calcitonin directly impair or inhibit osteoclast functions and induce the apoptosis of osteoclasts[8], while estrogen and SERMs have agonistic effects on intracellular estrogen receptors resulting in increasing estrogen activity and a decrease in osteoclast survival which increases bone mineral density (BMD)[9]. Denosumab is a monoclonal antibody against RANKL that prevents RANKL from interacting with the RANK receptor on osteoclast precursor cells, thereby inhibiting osteoclastogenesis[10]. Strontium ranelate has both anti-catabolic and anabolic effects by interacting with the RANKL pathway[11] and stimulating β-catenin in Wnt-signaling pathway which promotes osteoblast activity[12], respectively. The anabolic drugs induce

bone formation by activating the proliferation and inhibiting the apoptosis of osteoblasts[13]. Teriparatide (recombinant parathyroid hormone) is currently the only FDA-approved anabolic agent[1]. An alternate anabolic therapy currently in development is an antibody to sclerostin, the product of the *SOST* gene, which is secreted by osteocytes and promotes bone formation by osteoblasts. In a clinical study, administration of the anti-sclerostin antibody with exercise was shown to increase bone mass in patients by attenuating the antagonistic activity of sclerostin on canonical Wnt signaling, resulting in increased bone formation markers and decreased bone resorption markers[14].

Osteoclast differentiation and bone resorption

Osteoclasts are multinucleated cells derived from the hematopoietic stem cell lineage and function in bone degradation and resorption. The number and differentiation of osteoclasts is regulated by osteoblasts and osteocytes, which secrete macrophage colony-stimulating factor (M-CSF) and RANKL[15]. RANKL binds to RANK receptors on osteoclast precursors, and together with the action of M-CSF, stimulates osteoclast proliferation and differentiation and leads to an increase in osteoclast numbers[16]. In an *in vitro* study using the MLO-Y4 osteocytic cell line, M-CSF and RANKL expression were identified which were localized to the cell surface and to cytoplasmic processes[17]. Isolated osteocytes were also shown to express greater amounts of RANKL than osteoblasts and bone marrow stromal cells[15]. Osteoprotegerin (OPG) is also secreted from osteoblasts and osteocytes and acts as a decoy receptor for RANKL to inhibit osteoclastogenesis[17].

The differentiation of osteoblasts into osteocytes

Osteoblasts differentiate from osteoprogenitor cells or pre-osteoblasts, which are derived from the mesenchymal stem cells. Osteoblasts function in protein matrix secretion for bone generation[18]. This process is regulated by growth factors, hormones, and transcription factors (as shown in Figure 1)[19]. After completion of proliferation and differentiation, some osteoblasts change to become quiescent bone-lining cells or apoptotic cells, or alternatively, become embedded in the bone matrix and differentiate further to become osteocytes[5,20]. Several key proteins expressed in osteoblasts are shown in Table 1.

During osteocyte differentiation (osteocytogenesis), cell motility is arrested and the cells become embedded in the secreted bone matrix and undergo alteration in cell morphology [21]. During the process of osteocyte differentiation, actin cytoskeletal rearrangement leads to changes in cell shape from round to stellate or dendritic[22,23]. Concomitant with morphological changes, there is a significant decrease in the expression and secretion of several osteoblast-related proteins, including collagen type I, alkaline phosphatase, osteocalcin, and bone sialoprotein[24]. In addition, there is an increase in the expression of intracellular proteins that are unique to osteocytes, such as dentin matrix protein 1 (DMP1), matrix extracellular phosphoglycoprotein (MEPE) or sclerostin (SOST), as listed in Figure 2. The functions of these proteins are summarized in Table 2.

The biology of osteocytes

Osteocytes make up 90% of the total number of bone cells dispersed in the bone matrix. Unlike the morphology of osteoblasts, which are cuboidal in shape, mature osteocytes are stellate in shape and contain multiple cytoplasmic processes[23]. Osteocytes are deeply embedded in the bone matrix where they reside within nests called lacuna. Small channels known as canaliculi contain the osteocyte cytoplasmic processes. Both lacuna and canaliculi form the lacuna-canalicular system. Osteocytes maintain a distance of 50-80 nm from their cell bodies/cytoplasmic processes to the walls of their lacuna or canaliculi[25]. These spaces are filled with periosteocytic fluid, which is essential for metabolite transport for cell viability[26] and fibers for bridging osteocytes processes to the canaliculi walls[25]. The osteocytes in lacuna are surrounded by collagen type I. The formation of cytoplasmic processes depends on the cleavage of surrounding collagen type I by membrane-type matrix metalloproteinase-1 (MT1-MMP; MMP-14)[27-29]. In support of this, osteocytes from MT1-MMP-deficient mice showed shorter and fewer numbers of cellular processes than WT mice due to inadequate cleavage of the surrounding collagen type I[29].

The communication among several cell types is called multicellular syncytium (Figure 3)[30]. The cytoplasmic processes of osteocytes can contact the bone marrow, where they stimulate osteoclast differentiation. The cytoplasmic processes can also extend to the bone surface where they directly contact osteoblasts to promote bone formation[31,32]. The osteocyte cell body is polarized and the surface facing the

calcified matrix has shorter and thicker cytoplasmic processes with fewer organelles. In contrast, the cell surface facing the vascular space contains longer and thinner processes which are enriched with microtubules and microfilaments. These cytoplasmic processes are important in cell-cell communication via gap junctions at the tips of cytoplasmic processes. Connexin 43 is a major protein expressed at gap junctions, which allows cell-cell signaling of molecules smaller than 1.2 kDa[23].

Osteocytes also play an important function in mechanical stress detection and biochemical stimuli response[33]. Mechanical loading affects osteocytes by altering fluid flow along the lacuna-canalicular system[34]. Alteration of the flow of interstitial fluid in canaliculi results in deformation of the osteocyte plasma membrane. As a result, several intracellular signaling pathways and signaling molecules are activated and secreted. If there is a deficiency in mechanical loading, such as in an astronaut exposed to weightlessness, the secretion of osteoclast-inhibitory signals is decreased and pro-osteoclastogenesis signals are increased leading to a higher number of osteoclasts. When osteocytes respond to mechanical forces, they release prostaglandin E_2 (PGE_2) which stimulates osteoblast recruitment from the bone marrow and activates the Wnt/β-catenin signaling pathway[35]. Osteocytes also respond to mechanical loading by secreting nitric oxide, a stimulator of bone formation[36,37]. Bone formation is the physiological response to mechanical stress, whereas bone resorption is the reaction to unloading or skeletal disuse[36].

Osteocytes are also indirectly involved in osteoclastogenesis by stimulating osteoblasts to secrete RANKL, M-CSF[38] and osteoprotegerin (OPG)[39]. Osteocytes are also able to produce RANKL, M-CSF, and OPG, which can have a direct effect in regulating osteoclastogenesis[40]. Mechanical stimulation inhibits the apoptosis of osteocytes and increases osteocyte viability[41]. In addition, the apoptosis of osteocytes regulates osteoclast activity[42]. When micro-damage of bone occurs, osteocyte apoptotic bodies are able to activate osteoclastogenesis. This process is RANKL independent, but involves the tumor necrosis factor (TNF)-α[43].

When osteocytes are defective in function, sclerosteosis can occur. Sclerosteosis is a life-threatening pathology due to a mutation in the *SOST* gene, which encodes sclerostin in osteocytes. Sclerostin

produced by osteocytes counteracts Wnt signaling in osteoblasts by competitively binding to low-density lipoprotein receptor-related proteins (LRP) 5/6 and leading to the inhibition of osteoblastic-mediated bone formation. Therefore, a decrease in sclerostin production results in the exaggeration of osteoblastic bone formation. The common features in sclerosteosis patients are expansion of the jaw and facial bones and thickening and sclerosis of the skull. These pathological conditions result in the entrapment of cranial nerves and an increase in intracranial pressure, which can result in impaction of the brainstem and leads to death[44].

The arrangement of osteocyte cytoplasmic processes

The cytoplasmic processes of osteocytes are important in intercellular communication between osteocytes, osteoclasts, osteoblasts, or lining cells on the surface of bone[45]. Osteocyte processes are formed by reorganization of actin cytoskeleton[23]. Several actin-bundling proteins, such as CapG, Capzb, destrin, E11/gp38, α-actinin and fimbrin were detected in osteocytes. E11/gp38 regulates the dynamics of actin filaments by effecting the formation of cytoplasmic processes[46]. E11/gp38 interacts with the ezrin-radixin-moiesin (ERM) complex, which activates the downstream pathway of RhoA GTPase to regulate the dynamics of actin cytoskeleton[47].

Guanosine triphosphate (GTP)-binding proteins of the RhoGTPase family, such as Rho, Rac and Cdc42, play vital roles in many intracellular activities, including; cell migration, synaptic development, generation of dendritic spines, endocytosis, and the rearrangement of actin cytoskeleton[48-50]. These GTPases are inactive when bound to guanosine diphosphate (GDP). Guanine nucleotide exchange factors (GEFs) promote the dissociation of GDP and the binding of GTP to GTPases. Subsequently, GTPases are activated when bound to GTP[51,52]. The activated RhoGTPases bind effector molecules which are specific to selective Rho family members[31,53]. Consequently, signal transduction occurs from extracellular stimuli to activate intracellular pathways[48,54].

A novel GEF protein, Kalirin

In mammalian cells, the GTP-exchange factor proteins (GEFs) proteins are subdivided into 3 classes; Dbl homology-pleckstrin homology (DH-PH) domain, CDM and Zizimin homology (CZH) proteins, and DOCK-180 related proteins[50]. Almost all GEFs contain pleckstrin-homology (PH) domains. The function of the GEF domain is to catalyze the exchange reaction of GDP to GTP[55]. Different GEFs can activate more than one GTPase, while others can activate the same GTPases[55,56].

Kalirin is a multi-domain GEF protein belonging to the family of Dbl homology-pleckstrin homology proteins and contains two DH-PH domains. It is encoded by the *Kalrn* gene which undergoes alternative mRNA splicing, resulting in multiple isoforms[57], such as Kalirin-7, Kalirin-9, and Kalirin-12. Kalirin-9 and Kalirin-12 are highly expressed in developmentally embryonic stages. Their expression substantially decreases in adults and is correlated with an increase in the expression of Kalirin-7[58]. Kalirin-7 is the predominant isoform found almost entirely in postsynaptic terminals in the central nervous system[58]. The expression of Kalirin-7 is positively correlated with the formation of neuronal dendritic spines[58,59] and the density of glutamatergic synapses in hippocampal pyramidal neurons[58]. The expression of Kalirin-7 in Sprague–Dawley rats is extremely low during the first 7 days after birth and then increases significantly after 2 weeks of age[60,61].

Kalirin has several functional domains as shown in Figure 4[62]. The sec14 domain is involved in lipid interactions[62]; the spectrin-like repeat regions interact with several proteins, such as peptidylglycine α-amidating monooxygenase[63], inducible nitric oxide synthase[64], and Huntingtin-associated protein 1[65]. The N-terminal GEF domain binds to Rac1[66,67] and RhoA[68]. Kalirin-9 and Kalirin-12 isoforms are longer than Kalirin-7 and both contain a second C-terminal GEF-domain, which is active against RhoA[66,67]. RhoGEFs contain the Dbl-homology (DH) domain followed by a pleckstrin homology (PH) domain. The GEF binding site for GTPases is on the DH domain, while the PH domain constitutes the catalytic activity for the DH domain[69]. The PDZ domain targets Kalirin to specific locations in the cells and mediates assembly of the multi-protein complexes[68]. Kalirin-12 is the largest Kalirin isoform and also has a C-terminal immunoglobulin-fibronectin III (Ig-FNIII) domain and a serine-threonine (Ser-Thr) kinase

domain[70-72]. Although the functions of Kalirin are still largely unknown, Kalirin has been shown to be involved in the outgrowth of axons[67] and the formation of lamellipodia[73] and filopodial neurites[67]. Kalirin has been shown to be expressed in several tissues, such as neurons, liver, muscles, heart, and endocrine cells. In neurons, overexpression of Kalirin-7 resulted in an increase in the density, size of dendritic spines, and the number of synapses[74], while Kalirin-9 in cortical neurons induced the lengthening of neurites and had an influence on the morphology of neurons[67]. In addition, Kalirin-12 has been shown to interact via its Ig-FnIII region with the dynamin GTPase and affect actin cytoskeleton reorganization and endocytic trafficking[70].

Until recently, the skeletal role of Kalirin was unknown. Recent studies from Dr. Bruzzaniti's laboratory have shown that Kalirin is expressed in osteoclasts and osteoblasts. Importantly, female mice lacking the *Kalrn* gene (Kal-KO) have 45% less trabecular bone mass by 14 weeks of age[75], whereas male Kal-KO mice exhibit 19% bone loss. These findings suggest that Kalirin plays a role in the regulation of bone mass. Furthermore, studies from Dr. Bruzzaniti's laboratory suggest that the bone phenotype of Kal-KO mice is in part due to defects in the function of both osteoclasts and osteoblasts. However, the role of Kalirin in the function of osteocytes remains to be determined. Given that Kalirin can influence actin remodeling, dendritic spine formation and the synapses of neurons, it was hypothesized that Kalirin regulates the cytoplasmic processes of osteocytes, which may affect their ability to communicate with each other and to regulate the functions of osteoblasts and osteoclasts.

MATERIALS AND METHODS

1. Generation of Kalirin Knockout Mice

Kalirin global knockout (Kal-KO) mice were generated by removing exon13 of the *Kalrn* gene. Exon 13 encodes the spectrin region, which is a common region of all Kalirin major isoforms[76]. LoxP was introduced into the mice genome and flanked by loxP upstream and downstream of exon13. LoxP is a specific 34 base pair sequence having an 8-bp core sequence and two 13-bp inverted repeats. Cre recombinase is an enzyme recombining two loxP sites. The Cre-loxP recombination is able to delete loxP-flanked sequences. The Cre gene and loxP site are not naturally present in the mammalian genome. They are separately developed and then crossed to generate Cre-lox stain. Consequently, breeding of mice containing the Cre gene under control of the housekeeping gene promoter, hypoxanthine phosphoribosyltransferase 1 (HPRT) with *Kalrn* loxP mice results in progeny that lack all the major Kalirin isoforms in all tissues in mice. For all experiments, WT littermate mice were used as controls [62].

2. Isolation of primary osteocytes from mice

For the isolation of osteocytes from WT and Kal-KO mice, long bones (femurs and tibias) from the posterior legs of mice were collected in sterilized phosphate buffer saline (PBS). Soft tissue and periosteal tissue were removed by scraping. Both ends of tibias and femurs, including the growth plates, were removed. The cortical bone was separated from bone marrow by flushing with sterilized PBS (HyClone Laboratories, Inc., South Logan, Utah, USA) (Figure 5), followed by cutting into small pieces. The remaining soft tissue and bone marrow was removed by incubating in 5 ml of 300 collagenase digestive units (CDUs)/ml collagenase from *Clostridium histolyticum* type IA (Sigma-Aldrich Co. LLC, St. Louis, Missouri, USA) in α-Minimum Essential Medium (MEM) for 30 minutes in each digestion at 37°C under shaking conditions (200 rpm). The procedure was repeated 3 times, while the first fraction was discarded. After each sequential digestion, suspended cells were separated from bone pieces and collected by centrifugation. The bone pieces were washed 3 times with PBS. Then, they were alternatively incubated in 5 ml of ethylenediaminetetraacetic acid (EDTA) solution (Fisher Scientific, Pennsylvania, USA) and collagenase type IA another 6 times for osteocyte isolation[77]. The digest solution was centrifuged at 2000 rpm for 5 minutes. Cells from fractions 2-5 were plated in osteoblast-culturing medium that consists of α-Minimum Essential Medium (α-MEM) (HyClone Laboratories, Inc., South Logan, Utah, USA) with L-

glutamine supplemented with 10% (v/v) fetal bovine serum (FBS) (BioWest, Logan, Utah, USA) and 100 U/ml penicillin/100 µg/ml streptomycin (Lonza Walkersville, Inc., Walkersville, Maryland, USA). The cells from fractions 7-9 were re-suspended in 10% serum-osteocyte culturing medium, which consists of α-MEM with L-glutamine supplemented with 5% (v/v) FBS, 5% (v/v) bovine calf serum (BCS) (HyClone Laboratories, Inc., South Logan, Utah, USA) and 100 U/ml penicillin/100 µg/ml streptomycin, and plated in petri dishes coated with 0.01% calf skin collagen type I and grown for 1 month. The length and number of cytoplasmic processes were then observed under the microscope (Leica DMI4000B, Wetzlar, Germany). Wilcoxon rank sum tests were performed to analyze the data between the WT and Kal-KO groups with a 5% significance level. The remaining cortical bones were washed in sterilized PBS and crushed after freezing in liquid nitrogen. The crushed bone was submerged in Trizol (Life Technologies Corporation, Carlsbad, California, USA) and kept in -80°C for RNA extraction.

3. Scanning electron microscope analysis of osteocyte morphology

Mice long bones were isolated. Bone samples embedded in methyl methacrylate (MMA) were polished and etched for 20 seconds by immersing each specimen in 9% phosphoric acid. Immediately following etching, each section was immersed in bleach for 5 minutes, followed by 1-2 seconds in dH_2O. The sections were placed in a desiccator overnight and mounted on aluminum stubs using double-sided tape. The specimens were then sputter-coated with 3-5 nm of gold palladium at 2.5kV at 20mA for 105 seconds with a Polaron E5000S and then viewed on the JSM JEOL-6390LV scanning electron microscope (JEOL USA Inc., Massachusetts, USA) operated at an accelerating voltage of 5kV.

4. Osteocyte staining

Long bones from 14 week-old mice were isolated, cleaned, and then submerged in 1% basic fuchsin and 40% ethanol for 4 weeks. They were then immersed in copious amounts of tap water for 48 hours. The specimens were dehydrated, cut, and ground 50 µm thick and mounted on glass slides[78]. A number of osteocytes in the sections were observed under the microscope and counted from representative pictures that were taken from at least 5 different areas from one section. A total of 3 sections per bone specimen

were examined. The number of osteocytes in the WT and Kal-KO bone groups was statistically compared by Mixed-model ANOVA at a 5% significant level.

5. Culturing of the osteocyte cell line (MLO-Y4)

MLO-Y4 cells (murine long bone osteocyte Y4) were derived from the long bones of transgenic mice[79]. MLO-Y4 cells were grown in 5% serum-osteocyte culturing medium in an incubator at 37ºC with 5% CO_2. When the cells were 80% confluent, they were washed twice with PBS and detached using a 0.05% trypsin/0.44 mM EDTA solution (Life Technologies Corporation, Carlsbad, California, USA) at 37ºC for 5 minutes. The action of trypsin/EDTA was neutralized by adding osteocyte-culturing medium, and the cell suspension was centrifuged at 2000 rpm for 5 minutes at 4°C. The cell pellet was re-suspended with fresh culturing medium and plated on 0.01% (w/v) collagen calfskin (Sigma-Aldrich Co. LLC, St. Louis, Missouri, USA) coated petri dishes.

6. Plasmid purification

Plasmid expression constructs for several of Kalirin's functional domains were kindly provided by R.E. Mains, University of Connecticut Health Center, Connecticut, USA. Schematic representation of their domain structure is shown in Figure 6A. The accession number for Kalirin is 032062.2. The pEGFP.HisMyc.Kal-kinase construct containing the EGFP domain (238 amino acids (aa)), a histidine tag (HHHHHH) followed by a myc tag (EQKLISEEDL), and the kinase domain of Kalirin-12 (aa 2632-2959). A pCMS.HisMyc.Kal-kinase.EGFP construct contained the histidine and myc tags as well as the Kalirin-12 kinase domain but GFP was under the control of a separate promoter and was co-expressed with Kal-kinase in cells. The size of inserts is shown in Figure 6B.

Five microlitres of each cDNA were added into one tube Oneshot Top10® (Life Technologies Corporation, Carlsbad, California, USA). The Oneshot Top10 is commercial competent cells (*Escherichia coli)* with high efficiency cloning and plasmid propagation. The mixture was incubated on ice for 30 minutes, followed by heat shock in a water bath at 42ºC for 30 seconds and then suddenly placed on ice for 2 minutes. Super Optimal broth with Catabolite repression (S.O.C) 250 µl was added

into the mixture and incubated at 37°C for 1 hour at 225 rpm in the shaker incubator. Then, 200 µl of cultured solution was spread on Luria-Bertani (LB) agar plates (DOT Scientific Inc., Burton, Michigan, USA) containing the 100 µg/ml ampicillin or 100 µg/ml kanamycin, depending on the types of cDNA and incubated overnight at 37°C. The single colony was picked and inoculated in 10 ml LB media with antibiotics and incubated at 37°C 200 rpm in the shaker incubator overnight. The culture was diluted in 250 ml fresh LB broth and cultured under the same condition. Bacteria were then harvested by centrifugation at 6000 x g for 15 minutes at 4°C. Plasmids were purified by QIAGEN plasmid mini kit (QIAGEN, Hilden, Germany). The bacteria pellet was thoroughly re-suspended into 50 ml of re-suspension buffer, and then mixed with 50 ml lysis buffer and incubated at room temperature. This solution was vigorously mixed with 50 ml chilled neutralization buffer to promote the precipitation of genomic DNA, proteins, and cell debris and incubated on ice for 30 minutes. Then the solution was centrifuged at 20000 x g for 30 minutes at 4°C. The columns were prepared by loading 10 ml equilibration buffer through the column due to gravity to reduce surface tension. The filter sheets were placed on top of the column. The supernatant containing plasmid DNA was loaded into the column and filtrated by gravity flow. All contaminants were washed out using 60 ml wash buffer. The DNA was eluted with 15 ml elution buffer. The DNA was precipitated by adding 10.5 ml room-temperature isopropanol into the eluted DNA, mixing vigorously, and centrifuging at 15000 x g for 30 minutes at 4°C. The DNA pellet was washed with 5 ml room-temperature 70% ethanol and centrifuged at 15000 x g for 10 minutes. Finally, the pellet was eluted in Tris-EDTA (TE) buffer pH 8.0 at 4°C overnight and kept at -20°C.

7. Transient expression of Kalirin cDNA in MLO-Y4 cells

Three million MLO-Y4 cells were cultured in collagen-coated petri dishes to obtain 80-90% confluence within 24 hours. They were trypsinized and washed with cold Ca^{2+}/Mg^{2+}-free PBS. The cell pellet was re-suspended in 200 µl cold electroporation buffer (25 mM HEPES in PBS). The suspended cell solution (200 µl) was mixed with 100 µg DNA and incubated on ice for 15 minutes. The mixture was transferred into 2 mm plastic electroporation cuvettes. The cell-plasmid suspension was electroporated at 150 volts for 9 msec. The electroporated cells were left on ice for 5 minutes and then transferred into 10% serum-

osteocyte culturing medium in a collagen-coated petri dish and on a cover-slip in 6-well plates. The expression of Kalirin in MLO-Y4 was detected by Western blot analysis, while the morphology of the Kalirin-expressing cells was determined by microscopic analysis after immunofluorescent staining of cells.

8. Induction of cytoplasmic processes in MLO-Y4 cells

MLO-Y4 cells ($1x10^5$ cells) were cultured in the collagen-coated petri dishes and divided into 4 groups; one control group (cultured in osteocyte-culturing medium) and 4 treatment groups (cultured in osteocyte-culturing medium with 0, 25, 50, and 75 ng/ml nerve growth factor (NGF)-β or 50 mM potassium chloride (KCl) for 5 days. After treatment, the morphology of the cells was observed by microscopy. Alternatively, the cells were trypsinized, collected, and examined by Western blot analysis.

9. SDS-PAGE and Western blot analyses

MLO-Y4 cells over-expressing the Kal-kinase domain or treated with NGF or KCl were lysed in SDS buffer (100 mM HCl, 500 mM Tris pH8.0, 10% SDS (wt/v) containing 10 µg/ml leupeptin hydrochloride, 10 µg/ml aprotinin, and 10 µg/ml pepstatin), and sonicated for 2 minutes. The lysates were collected, centrifuged at 13,000 rpm for 5 minutes and the supernatant was collected. The amount of protein was estimated with the BCA protein analysis kit (Thermo Fisher Scientific Inc., Waltham, Massachusetts, USA) and 40 µg of protein was resolved by SDS-PAGE electrophoresis. Protein samples were mixed with loading buffer (62.5 mM Tris HCl pH 6.8, 2% w/v SDS, 10% glycerol, 50 mM DTT, and 0.01% bromophenol blue). All samples were boiled at 100°C for 5 minutes. The samples were loaded onto 4%-12% NuPAGE Bis-Tris gels and subject to electrophoresis with NUPAGE MOPS (or MES) SDS Running Buffer (Life Technologies Corporation, Carlsbad, California, USA). Molecular weight protein markers were added and proteins were resolved at 120 volts, 3.0 amperes for approximately 2.5 hours. The proteins were transferred to nitrocellulose membrane in MOPS NuPAGE transfer buffer (Life Technologies Corporation, Carlsbad, California, USA) with 20% methanol at 100 volts for 1 hour at 4°C. The membrane was washed with TBST solution (0.2 M Tris Base and 0.6 M NaCl at pH7.4 containing 0.1% Tween-20) for 5 minutes at room temperature. Non-specific proteins were blocked with

5% skim milk in TBST solution for 1 hour, shaking. Primary antibodies (Table 3) were diluted (1:1000) in TBST buffer. The membrane was incubated with the primary antibody overnight at 4°C. The membrane was then washed 3 times for 15 minutes each with TBST buffer. An anti-mouse antibody conjugated with horseradish peroxidase (HRP) was diluted 1:20000, while anti-rabbit HRP was diluted 1:10000 in the TBST buffer and incubated with the membrane for 1 hour at room temperature on the shaker. The membrane was washed 3 times for 15 minutes in TBST buffer and proteins were detected using the enhanced chemiluminescence (ECL) reagent (SuperSignal West Pico Chemiluminescent Substrate, Thermo Fisher Scientific Inc., Rockford, Illinois, USA) for 5 minutes according to the manufacturer's instructions. Membranes were exposed to X-ray film (Thermo Fisher Scientific Inc., Waltham, Massachusetts, USA) and developed.

10. Immunofluorescent staining

Cells on glass cover slips were washed twice with PBS and fixed with 10% formaldehyde in PBS for 15 minutes, followed by washing twice with PBS. The cells to be stained for actin filaments with rhodamine phalloidin were permeabilized by acetone treatment for 3 minutes, followed by washing twice with PBS. Non-specific proteins were blocked with blocking solution (0.1% bovine serum albumin (BSA), 0.05% saponin, and 5% goat serum) at room temperature for 30 minutes. The blocking solution was removed. Primary antibody, rabbit polyclonal anti-Kalirin antibody, was diluted 1:200 in the blocking solution. The cover slips were incubated for 2 hours at room temperature. They were washed 3 times with blocking solution. The fluorescent-conjugated secondary antibody was diluted 1:100 in the blocking solution. The cells were incubated for 1 hour at room temperature and protected from light. They were washed 3 times with PBS. Rhodamine phalloidin diluted in blocking solution (1:200) was added to cells on cover slips for 1 hour. Nuclei were labeled with Dapi diluted (1:600) in PBS. The cover slips were mounted with FluorSave medium (Calbiochem, Massachusettes, USA)

11. Isolation of RNA from bones and MLO-Y4 cells

For cell lines, the plate/flask was grown until 80% confluent and then washed, trypsinized, and centrifuged to collect the cells (Section 5). For cortical bones, the crushed bones in Trizol solution

(Section 2) were sonicated. The sample was then incubated at room temperature for 5 minutes to permit the dissociation of nucleoprotein complexes and centrifuged at 13,000 rpm for 10 minutes at 4°C. The supernatant containing RNA was collected in new microcentrifuge tubes. A phase separation was performed by adding 200 µl of chloroform into the RNA solution and centrifuged at 13,000 rpm for 15 minutes at 4°C. The top clear liquid with RNA was transferred into a new tube. To precipitate the RNA, 500 µl of absolute isopropyl alcohol was added, incubated at room temperature for 10 minutes, and centrifuged at 13,0000 rpm for 10 minutes at 4°C. The supernatant was discarded. The RNA pellet was washed with 1 ml of cold 75% ethanol, vortexed, and centrifuged at 7,500 rpm for 5 minutes at 4°C. The RNA was then re-suspended in 100 µl of RNase-free water. The mRNA was purified using the RNeasy® Mini Kit (QIAGEN Sciences Inc., Germantown, Maryland, USA). Any remnant genomic DNA in the RNA samples was degraded by digestion with DNase I (Applied Biosystems, Warringtons, UK) by incubation at 37°C for 30 minutes. Then, 5 mM EDTA solution was added into the RNA-DNaseI solution and incubated at 75°C for 5 minutes to remove excess DNaseI.

12. Generation of cDNA by reverse transcription reaction

Complementary DNA (cDNA) was generated using the Transcriptor First Strand cDNA Synthesis Kit (Roche Applied Science, Mannheim, Germany), which used the reverse transcriptase (RT) and oligo (dT_{18}) primers to convert mRNA to cDNA. For each reaction, 100 ng of mRNA was added. The solution was briefly centrifuged and then incubated on a thermal cycler (C1000, Bio-Rad Laboratories Headquarters, Hercules, California, USA) at 50°C for 60 minutes (for reverse transcriptase reaction with dNTPs) followed by heating at 85°C for 5 minutes (stop reaction) and at 4°C continually until the cDNA was stored at -20°C.

13. Quantitative Real-time Polymerase Chain Reaction

Quantitative polymerase chain reaction (QPCR) was used to quantify expression of mRNA from WT and Kal-KO osteocytes. Syber® green Gene Expression Master Mix (Applied Biosystems, Warringtons, UK) was used. A list of the genes examined is shown in Table 4. All oligonucleotide primers were validated against their appropriate targets by sequence comparison and by reverse-transcription PCR and agarose

gel electrophoresis before being used for QPCR. The *18S* RNA housekeeping gene was used as an endogenous control. In each QPCR reaction, 100 ng of cDNA was added. All samples were centrifuged to collect reagents and then run in the QPCR machine (Applied Biosystems Prism 7000 using STEP1 Software Solutions, Newbury Park, California, USA) in duplicate with the temperature profile: 50°C for 2 minutes, 95°C for 10 minutes, and 50 repeating cycles of 95°C for 15 seconds and 56°C for 1 minute. In all experiments, the threshold cycle (Ct) for each test gene was normalized against its respective endogenous controls. Real-time PCR was analyzed in fold changes in expression relative to wild-type osteocytes with ΔCt values of the sample and reference gene using the formula $2^{-\Delta\Delta Ct}$.

RESULTS

1. Differential expression of Kalirin isoforms in primary osteocytes

The role of Kalirin on osteocyte morphology and function was examined. First, the mRNA expression level for the Kalirin isoforms in cortical bone was examined. The isolated mRNA of osteocytes from cortical bone of mice tibias and femurs was reverse transcribed to cDNA (see section 11 and 12). The expression of Kalirin-7, Kalirin-9 and Kalirin-12 was examined by QPCR using isoform-specific oligonucleotide primers. In primary osteocytes, Kalirin-9 mRNA was found to be more abundant than Kalirin-12, followed by Kalirin-7 mRNA (Figure 7A).

The mRNA expression level of the Kalirin isoforms was also examined in MLO-Y4 cells, an osteocytic cell line developed from murine long bones which was used for *in vitro* studies of Kalirin (see section 5). All 3 major isoforms of Kalirin were also detected in MLO-Y4 cells. Similar to primary osteocytes, Kalirin-9 mRNA was more abundant than Kalirin-12, while Kalirin-7 mRNA levels was found to be the least abundant of the Kalirin isoforms (data was not shown).

Kalirin protein levels in MLO-Y4 cells was also examined by Western blotting using an antibody that detects all major Kalirin isoforms (anti-sec14 antibody) or using a Kalirin-12-specific antibody (Kal12) (provided by Drs. Main and Eipper, University of Connecticut Health Center, CT). Western blot analysis revealed the expression of several Kalirin isoforms in MLO-Y4 cells (Figure 7B). Based on the predicted molecular weight of the isoforms, these results indicated that Kalirin-7 protein levels were more abundant in MLO-Y4 cells than Kalirin-9.

2. Kalirin is localized to the cytoplasmic extensions of osteocytes

To further examine the expression of Kalirin in osteocytes, immunofluorescent staining of Kalirin in primary osteocytes and MLO-Y4 cells was performed. Primary calvarial osteoblasts were used as a positive control in these studies. Cells were plated on coverslips then fixed and labeled with an antibody to Kalirin (rabbit polyclonal anti-Kalirin antibody, Millipore Corporation, Billerica, MA, USA) (green). Cells were also co-stained for actin filaments using rhodamine phalloidin (red) or for nuclei using DAPI (blue) (Figure 8-10). In osteoblasts, Kalirin was found to be expressed at the perinuclear region and was

localized to actin-rich fibers/tubules that extended radially from the nucleus to the cell periphery. However, Kalirin was not detected in circular actin-rich fibers that surrounded the nucleus (Figure 8). In primary osteocytes, Kalirin was also expressed at the area close to the nucleus and was localized to actin-rich cytoplasmic processes, often extending out to the tips of the processes in contact with an adjacent cell (Figure 9). Similar to osteoblasts, Kalirin was detected at the perinuclear area and along linear actin-rich fibers in MLO-Y4 cells (Figure 10).

3. Osteocyte morphology is altered in the absence of Kalirin

The role of Kalirin in regulating the morphology of the cytoplasmic processes in osteocytes was then examined *in vivo* and *in vitro* using WT and Kal-KO mice. Kal-KO mice were previously generated[80] and lacked all three major Kalirin isoforms, as well as some minor isoforms[81]. First, the femurs of 14 week-old mice Kal-KO and WT were isolated and the bones cleaned of tissue. The bones were stained with basic fuchsin, which stains the cell nucleus, and then sectioned and imaged (Figure 11A). The osteocyte cell bodies embedded in lacuna appeared dark red in color and multiple cytoplasmic processes were observed (Figure 11A). The number of osteocytes were counted and compared between WT and Kal-KO mice (n=3 in each group) from 5 random areas of bone sections. However, the number of osteocytes in WT (93.3±3.9) and Kal-KO (83.8±4) bones were not found to be significantly different ($p>0.05$) as determined by mixed-model ANOVA statistical analysis (Figure 11B). The number and morphology of osteocytes in cortical bone from Kal-KO and WT mice was also examined by acid-etching of plastic-embedded bones specimens, followed by imaging using a scanning electron microscope (SEM). Although extensive cytoplasmic processes were observed in both WT and Kal-KO bones (Figure 12), no qualitative differences between Kal-KO and WT osteocytes were apparent, and further quantitative analyses were not possible with these specimens due to the large number of interconnected cytoplasmic extensions present.

To better examine the effects of Kalirin deletion on osteocyte morphology, primary osteocytes from Kal-KO and WT cortical and trabecular bones were used. Cells were isolated from the tibias and femurs of WT and Kal-KO mice by sequential collagenase digestion and then cultured *in vitro* for up to 1 month on

collagen-coated dishes. Osteocytes were then examined by microscopy for differences in length and number of cytoplasmic processes (Figure 13A). The average number of cytoplasmic processes detected in WT osteocytes (4.69±0.3) was significantly higher ($p<0.05$) than the average number of cytoplasmic processes found in Kal-KO osteocytes (3.32±0.21). In addition, the length of cytoplasmic processes of WT osteocytes (85.4±3.6 μm) was found to be significantly higher than the cytoplasmic processes of Kal-KO osteocytes (79.5±4.6 μm) (Figure 13B). These findings revealed that Kalirin played a crucial role in controlling the length and number of cytoplasmic processes of osteocytes.

4. Kalirin regulates mRNA levels of osteocyte genes

Given that all 3 major Kalirin isoforms were detected in osteocytes and that osteocytes lacking Kalirin isoforms exhibited defects in the number and length of cytoplasmic processes, the role of Kalirin in regulating the function of osteocytes was examined. To this end, QPCR analysis of known osteocyte marker genes was performed. RNA was isolated from cortical bone of tibias and femurs of WT and Kal-KO mice, reverse transcribed and subject to QPCR analysis using oligonucleotide primers to known osteocyte genes. The expression of *18S* RNA was used as the endogenous control and results for Kal-KO osteocytes were normalized to WT levels (set as 1.0) (Figure 14). Statistical analysis of QPCR results from the WT and Kal-KO bone groups was performed by Wilcoxon rank sum tests (Figure 14).

E11/gp38 is the earliest osteocyte-specific protein to be expressed in osteocytes as they become embedded in osteoid. MEPE and PHEX are also markers for osteocytes embedded in osteoid, and also function in regulating phosphate homeostasis[82]. QPCR analysis revealed that *MEPE* mRNA levels were significantly decreased ($p<0.05$) in Kal-KO bones compare to WT bones (Figure 14), whereas *E11/gp38* mRNA levels appeared normal. Dmp1 is also expressed in early mineralizing osteocytes and is a marker of osteoblasts transitioning into osteocytes. Similar to *E11/gp38*, the expression of *Dmp1* mRNA was not found to be significantly different in Kal-KO osteocytes. Therefore, these findings suggest that in the absence of Kalirin, the differentiation of osteoblasts to early osteocytes appears normal, but osteoid formation and mineralization by osteocytes may be reduced.

IGF-1 is known to enhance the differentiation of late osteoblasts[83] and to play a role in longitudinal bone growth[84]. The expression of *IGF-1* was found to be significantly lower in Kal-KO bones than WT, which also implied the impairment of early osteocyte formation. *FGF23* and *SOST* are both expressed in mature osteocytes. FGF23 plays a role in phosphate metabolism while the product of the *SOST* gene, sclerostin, is an inhibitor of Wnt signaling and inhibits the proliferation and differentiation of osteoblasts[85]. QPCR analysis revealed no change in *FGF23* mRNA levels. However, *SOST* mRNA levels were significantly lower in Kal-KO than WT bones. ER-α and ER-β are known to be strongly expressed in cortical bone and cancellous bone, respectively[86]. The expression of *ER-α* mRNA in osteocytes was significantly decreased ($p<0.05$) in Kal-KO mice. On the contrary, the expression of *ER-β* mRNA in Kal-KO bones was significantly increased ($p<0.05$) compared in WT bones. Finally, the ratio of RANKL and OPG is critical for the regulation of osteoclast differentiation. A significant decrease in *OPG* mRNA ($p<0.05$), but not *RANKL* mRNA ($p>0.05$) levels, was detected in Kal-KO bones compared to WT bones, suggesting a decrease in the RANKL/OPG ratio in Kal-KO mice, which would likely affect osteoclast number in these mice, consistent with unpublished studies from Dr. Bruzzaniti's laboratory.

5. Induction of cytoplasmic processes in MLO-Y4 cells regulates Kalirin, Rac1 and RhoA

Examination of osteocyte morphology revealed Kal-KO osteocytes had shorter and fewer cytoplasmic processes than WT osteocytes, while immunofluorescent staining showed that Kalirin was expressed along the cytoplasmic processes of osteocytes. To begin to understand the intracellular signaling events leading to changes in cytoplasmic process formation, and to confirm Kalirin's role in this process, two novel *in vitro* approaches to induce cytoplasmic process extension in ML0-Y4 cells were developed. Kalirin had previously been shown to play a role in neuronal dendrite formation downstream of nerve growth factor (NGF)-β[87]. Furthermore, dendritic spine elongation in neurons was promoted using high extracellular levels of potassium chloride (KCl), which led to neuronal cell depolarization[88]. Therefore, cytoplasmic process elongation in MLO-Y4 cells was examined following treatment with NGF (0, 25, 50, 75 ng/ml) or 50 mM KCl for 5-7 days. The NGF and KCl concentrations used and the time of treatment for these studies were pre-optimized for maximal effects on cytoplasmic process elongation (data not shown). Following cell treatment, the protein level of the Kalirin isoforms was determined by Western

blotting. In addition, the phosphorylation of extracellular regulated kinase (ERK), which was previously implicated in osteoblast signaling downstream of Kalirin (Huang *et al*. unpublished data), was examined. As shown in Figure 15, the cytoplasmic processes of MLO-Y4 cells were significantly lengthened after 5-7 days of treatment, with 75 ng/ml NGF and 50 mM KCl inducing maximal morphological responses. Western blot analysis using isoform-specific antibodies to Kalirin revealed a dose-dependent increase in Kalirin-7 and Kalirin-12 in cells treated with NGF (Figure 16). Consistent with the increase in Kalirin, the level of total RhoA was increased, whereas Rac1 protein levels remained the same. In contrast, Kalirin-7, Kalirin-12 and RhoA protein levels were reduced in MLO-Y4 cells treated with KCl, compared to vehicle treated controls.

6. The Kalirin-12 kinase domain regulates cytoplasmic process formation in MLO-Y4 cells

To examine the mechanism of action of Kalirin in regulating cytoplasmic process formation, MLO-Y4 cells were electroporated to express Kalirin functional domain. Mammalian expression constructs encoding GEF1, GEF2, Ig/FnIII or the Kalirin-12 Ser-Thr kinase domain were used (see Figure 6). Two plasmid expression constructs for the Kalirin-12 Ser-Thr kinase domain were used; in Kal-kinase1, the GFP-tag was directly linked to the C-terminal end of the kinase domain, whereas in Kal-kinase2 the GFP expression was under the control of a separate promoter and was co-expressed with the kinase-domain (see Figure 6). Although all expression constructs generated protein products of the correct molecular weight in control non-osteocytic cells (data not shown), only the Ser-Thr kinase domain of Kalirin-12 was successfully expressed in the MLO-Y4 osteocytic cell line (Figure 17). The electroporation efficiency of Kal-kinase1 and Kal-kinase2 cDNA constructs was approximately 80% and 60% respectively (Figure 18). Following electroporation of Kal-kinase1 or Kal-kinase2 the morphology of MLO-Y4 cells was examined by microscopy. Changes in the actin cytoskeleton were observed by labeling with rhodamine phalloidin (red), while Kal-kinase expression was detected by virtue of the GFP tag. The pEGFP empty vector, which also expresses GFP, and non-electroporated cells were used as negative controls. As shown in Figure 18, MLO-Y4 cells expressing the Kal-kinase domain (green) exhibited changes in the appearance of their cytoplasmic processes (red), compared to empty vector or non-electroporated control cells. Specifically, short cytoplasmic processes with extensive branching were observed in MLO-Y4 cells

expressing the Kal-kinase domain (Figure 18; arrows), compared with the pEGFP empty plasmid or non-electroporated cells.

MLO-Y4 cells expressing the Kal-kinase1 and Kal-kinase2 cDNA expression constructs were also examined by Western blotting. The expression of Kal-kinase1 and Kal-kinase2 was determined using an antibody to the myc tag. We also examined if over-expression of the kinase domain affected Rac1 and RhoA protein levels, as well as the phosphorylation of ERK (pERK), which was reported to play a role in Kalirin signaling mechanisms[89]. Electroporation appeared to induce the phosphorylation of ERK compared to cells electroporated with pEGFP. Nevertheless, examination of MLO-Y4 cells expressing Kal-kinase1 and Kal-kinase2 showed a higher ratio of pERK to total ERK, compared to control electroporated cells. Similar to MLO-Y4 cells treated with increasing concentrations of NGF, no change in Rac1 levels was observed in cells expressing Kal-kinase1 or Kal-kinase2. Moreover, MLO-Y4 cells expressing the kinase domain of Kalirin-12 had higher levels of RhoA than control cells.

TABLES

Proteins	Functions
Alkaline phosphatase (ALP)	Marker of bone metabolism[90]
β-catenin	Involved in the differentiation of mesenchymal progenitor cells via the Wnt pathway[91]
Collagen type I	Marker for bone formation[92]
Core-binding factor alpha 1 (Cbfa1) or Runt-related transcription factor 2 (Runx2)	Required for the differentiation of mesenchymal stem cells into the osteoblast lineage and for embryonic bone formation[93] Is upregulated by BMP2 and Wnt pathways during osteoblast differentiation[93]
Keratocan	Regulation of cell proliferation and differentiation of osteoprogenitor linage cells[94]
Osteocalcin (OCN)	Marker of osteogenic maturation and bone turnover[95] Ca^{2+} binding protein[95]
Osteopontin (OPN)	Mediates binding between the bone matrix and the vitronectin receptors expressed in the sealing zone of osteoclasts[96]
Osteoprotegerin (OPG)	Negative regulation osteoclastogenesis[97]
Osterix	Involved in immature osteoblasts differentiation into pre-osteoblasts[98]
Receptor activator of nuclear factor kappa-B ligand (RANKL)	Cytokine secreted by osteoblasts that regulates osteoclast activation and differentiation[16]
Bone sialoprotein	Bone mineralization and bone growth[99] Marker of the late stages of osteoblast differentiation and the early stages of mineralization[99]

TABLE 1. Osteoblast signaling and regulatory proteins.

The table shows different proteins which are specifically expressed in osteoblasts, and their functions.

Proteins	Functions
Dentin matrix protein 1 (DMP1)	Cytoplasmic process formation[100] Binding to CD44, which interacts with adapter proteins that link to actin cytoskeleton[101] Regulates mineralization and mineral metabolism[102] Regulates the maturation of osteocytes and phosphate metabolism[103] Expressed in the pericellular matrix, cytoplasmic processes, osteocyte lacuna-canaliculi system and several parts of bone; metaphyseal primary trabeculae (bone modeling region) and secondary trabeculae (bone remodelling region) as well as cortical bone[104,105] Marker for the transitioning of osteoblasts into osteocytes[106] DMP1 is detected after osteopontin, osteocalcin and bone sialoprotein are activated[106]
Estrogen receptor α1	Involved in the responsiveness of osteocytes to mechanical stress and the apoptosis of osteocytes[107] Prevalently presented in the osteocytes in cortical bones[107]
Estrogen receptor β1	Involved in the responsiveness of osteocytes to mechanical stress and the apoptosis of osteocytes[107] Predominantly presented in the osteocytes in cancellous bone[107]
Fibroblast growth factor 23 (FGF23)	Regulates renal phosphate excretion[102] Regulates the level of phosphorus and Vitamin D metabolisms[108] Inhibits osteoblast maturation by disrupting the Wnt signaling pathway[109] FGF-23 is regulated by PHEX[108]
Matrix extracellular phosphoglycoprotein (MEPE)	Phosphate homeostasis[82] Inhibits bone formation[110] Regulates the mineralization process[111] Up-regulates osteoprotegerin (OPG)[112]
Phosphate-regulating gene with homology to endopeptidases on the X chromosome (PHEX)	Phosphate homeostasis[82] Regulates MEPE[113]
Podoplanin (E11/gp38)	A marker of embedded osteoid osteocytes[102] Regulated the dendritic and canaliculi formation[102]
Receptor activator of nuclear factor kappa-B ligand (RANKL)	Cytokine secreted by osteocytes that regulates osteoclast activation and differentiation[16]
Sclerostin (SOST)	Inhibits the proliferation and differentiation of osteoblasts[114] Stimulates the apoptosis of osteoblasts[115] Inhibits bone formation by antagonizing Wnt/β-catenin pathway[116,117] The impairment of this gene in mice leads to high bone mass[117]

TABLE 2. Osteocyte signaling and regulatory proteins.

Different proteins which are specifically expressed in osteocytes and their functions are summarized in the table.

Antibodies	Company	Concentration
Mouse monoclonal anti-Myc antibody (Clone 9E10)	Santa Cruz Biotechnology, Inc, Dallas, TX, USA	1:1000
Mouse monoclonal anti-green fluorescent protein (GFP) antibody (Clone JL-8); Living colors®	Clontech Laboratories, Inc.,Mountainview, CA, USA	1:1000
Rabbit polyclonal anti-Kalirin sec14 antibody (Clone CT301)	From RE. Mains and BA. Eipper, UConn, CT	1:1000
Rabbit polyclonal Anti-COOH terminus of kalirin-12 antibody (Clone Ab3225) [61]	From RE. Mains and BA. Eipper	1:1000
Rabbit monoclonal anti-P-p44/42 MAPK antibody (PhosphoERK)	Cell Signaling Technology, Inc., Danvers, MA, USA	1:1000
Rabbit polyclonal anti-ERK1 antibody (Total ERK)	BD Biosciences, San Jose, CA, USA	1:1000
Mouse monoclonal anti-Rac1 antibody (Clone 23A8)	Millipore Corporation, Billerica, MA, USA	1:1000
Rabbit polyclonal anti-Kalirin antibody	Millipore Corporation, Billerica, MA, USA	1:200
Rabbit polyclonal with horseradish peroxidase conjugated	Promega Corporation, Madison, WI, USA	1:10000
Mouse monoclonal with horseradish peroxidase conjugated	Promega, Corporation, Madison,WI, USA	1:20000

TABLE 3. Antibodies for Western blotting and immunofluorescent staining.

The table shows different antibodies and their concentrations for Western blot assays and immunofluorescent staining of primary osteocytes and MLO-Y4 osteocytic cells used in this study.

Primers	Primer sequences	Expression	Temperature (°C)	
			Melting	Annealing
18S	Forward: AGTCCCTGCCCTTTGTACACA Reverse: CGATCCGAGGGCCTCACTA	Housekeeping gene	60.5	56
Dentin matrix protein 1 (DMP1)	Forward: TCAGGACAGTAGCCGATCCA Reverse: TCCCCGATGGGTTTGTTGTG	Differentiating osteoblasts Early osteocytes [106] Highly expressed in osteocytes [46,82]	60	56
Fibroblast growth factor 23 (FGF23)	Forward: GTGTCAGATTTCAAACTCAG Reverse: GGATAGGCTCTAGCAGTG	Highly expressed in osteocytes [82,118,119] Low expressed in osteoblasts [118,119]	52	56
Estrogen receptor-α	Forward: CTCAACCGCCCGCAGCTCAA Reverse: GTAGGCGATGCCCGACTGGC	Growth plate cartilage [120] Strongly expressed in osteoblasts, osteocytes [86], and osteoclasts [120] in cortical bones	65	60
Estrogen receptor-β	Forward: ACCCTCACTGGCACGTTGCG Reverse: GGCTTGCGGTAGCCAAGGGG	Growth plate cartilage [121] Strongly expressed in osteoblasts and osteocytes in cancellous bone [86]	65	63
Matrix extracellular phosphoglycoprotein (MEPE)	Forward: TCAAGACAGCATTCACAAGGAC Reverse: GGAGGGCAGCACCATACC	Predominantly expressed in osteocytes No expression in osteoblasts [46,82,111,112]	58.8	56
Osteoprotegerin (OPG)	Forward: ACCCAGAAACTGGTCATCAGC Reverse: CTGCAATACACACACTCATCACT	Osteoblasts [97] Osteocytes [112]	59	56
Phosphate-regulating gene with homology to endopeptidases on the X chromosome (PHEX)	Forward: TGATGGAAGCAGAAACAG Reverse: CTTGGAAACTTAGGAGACC	Osteocytes [82,112]	52	56
Podoplanin (E11/gp38)	Forward: AGCCCAGTCCTAAGCATCCA Reverse: CGTGGCTCCTCAACTCATCG	Early osteocytes Osteoblasts differentiate into osteocytes [100]	60	56
Receptor activator of nuclear factor kappa-B ligand (RANKL)	Forward: TCCTGTACTTTCGAGCGCAC Reverse: CCAGAGTCGAGTCCTGCAAA	Osteoblasts [97] Osteocytes [112]	59	56
Sclerostin (SOST)	Forward: CCACAAAGACTGAAAGCCGC Reverse: TAACAATGCCTCTGGTCGGG	Restrictedly expressed in osteocytes [115]	59.75	56
Kalirin-7	Forward: GATACCATATCCATTGCCTCCAGGACC Reward: CCAGGCTGCGCGCTAAACGTAAG	Hippocampus and the cerebral cortex of the brain [122]	61	57
Kalirin-9	Forward: GCCCCTCGCCAAAGCCACAGC Reward: CCAGTGAGTCCCGTGGTGGGC	Growth cones of the axon and neurites[67]	62	59.5
Kalirin-12	Forward: CTTCATAGAACGCCGCAAGC Reverse: ACCTCAGGGGTTGTGGGATA	Neurons [61,122]	61	57.5

TABLE 4. Oligonucleotide primers used for QPCR.

The table shows the oligonucleotide primer sequences and their melting and annealing temperatures, including information regarding the expression of each gene in different tissues. These primers are specific to the selected genes.

	Genotype	Mean±SE	p-value
Number of processes	WT KO	4.69±0.3 3.32±0.21	0.0004
Length of processes	WT KO	85.4±3.6 79.5±4.6	0.0276
Number of osteocytes	WT KO	93.4±4.7 83.6±2.6	0.2243

TABLE 5. Analysis of osteocyte cytoplasmic processes from Kal-KO and WT mice.

The chart summarizes data comparing the number and length of cytoplasmic processes detected in cultured osteocytes from WT and Kal-KO mice. To determine the number and length of cytoplasmic processes, a total number of 68 WT and 78 Kal-KO osteocytes were examined from one preparation of cells isolated from mouse femur and tibia (pooled samples). Microscopic analysis revealed that Kal-KO osteocytes have significantly shorter and fewer cytoplasmic processes compared to WT osteocytes ($p<0.05$). The average numbers of osteocytes embedded in cortical bones from WT (6 independent bone sections) and Kal-KO (8 independent bone sections) mice, as determined by basic fuchsin-staining, are also shown. There is no statistic different in number of osteocytes between WT and Kal-KO groups ($p>0.05$). All data was analyzed using the Wilcoxon rank sum tests.

FIGURES

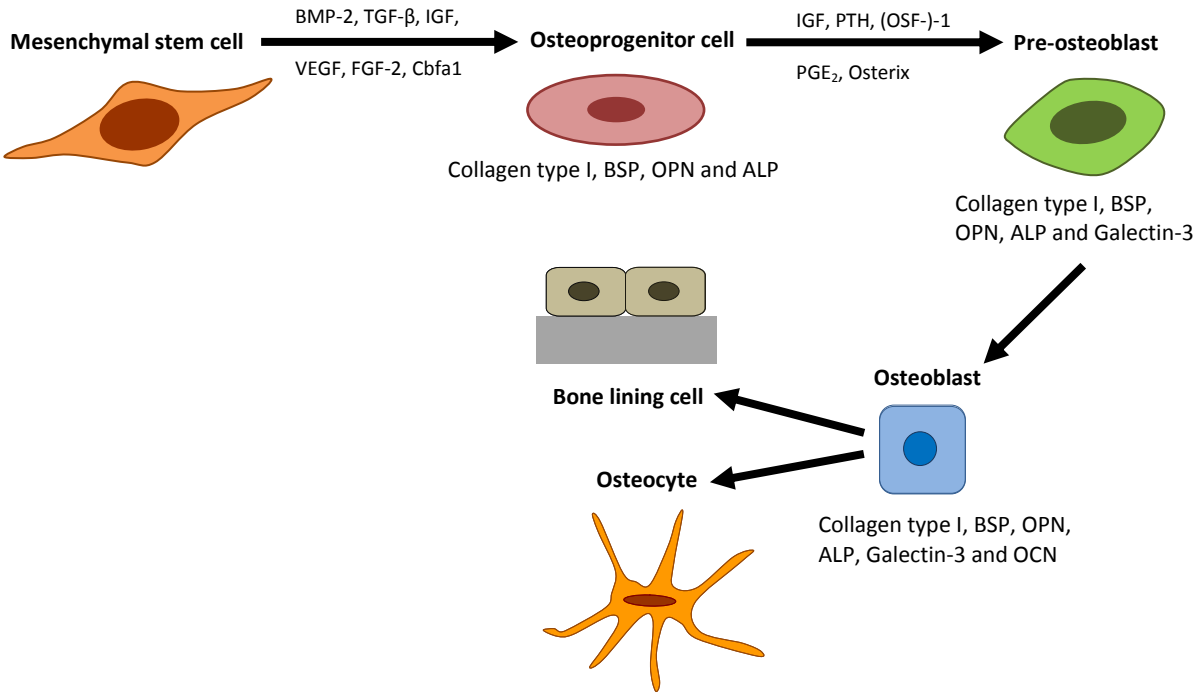

FIGURE 1. Schema for mesenchymal stem cell differentiation into osteoblasts.
Osteoblasts are specialized fibroblasts which are able to secrete and mineralize the bone matrix. They differentiate from mesenchymal stem cells. Osteoblast differentiation involves the interaction of transcription factors as well as endocrine, paracrine and autocrine factors. BMP-2 induces Cbfa1 activity in mesenchymal stem cells [123]. Cbfa1 directs mesenchymal stem cells to commit to an osteoblast pathway [124]. TGF-β regulates the proliferation of undifferentiated mesenchymal stem cells and the differentiation of osteoprogenitor cells [125]. Growth factors (BMP, TGF, IGF, VEGF and FGF) also support the recruitment and proliferation of osteoprogenitor cells [125].

Osteoprogenitor cells differentiate into pre-osteoblasts depending on several regulatory factors. Osterix is important to shifting bipotent osteoprogenitor cells from the chondrocytic lineage to the osteoblastic lineage [126]. IGF and PGE_2 promote the proliferation and differentiation of osteoprogenitor cells to pre-osteoblasts [127]. PTH balances the differentiation of osteoprogenitor cells by inhibiting the late stage of differentiation of osteoprogenitor cells to pre-osteoblasts [128]. Pre-osteoblasts differentiate into osteoblasts via an increase the activity of Cbfa1 and increases in the expression of collagen type I, BSP, OPN, ALP and Galectin-3, and begin to express OCN [123]. The mature osteoblasts further differentiate into either bone lining cells or osteocytes.

BMP: Bone morphogenic protein; TGF: Transforming growth factor; IGF: Insulin-like growth factor; VEGF: Vascular endothelium growth factor; FGF: Fibroblast growth factor; PTH: Parathyroid hormone; (OSF-)-1 osteoblast stimulating factor or pleiotrophin (PTN) or heparin-binding growth-associated molecules (HB-GAM), Cbfa1: Core-binding factor alpha 1 or Runt-related transcription factor 2 (Runx2); PGE2: Prostaglandin E2; BSP: Bone sialoprotein; OPN: Osteopontin; ALP: Alkaline phosphatase and OCN: osteocalcin.

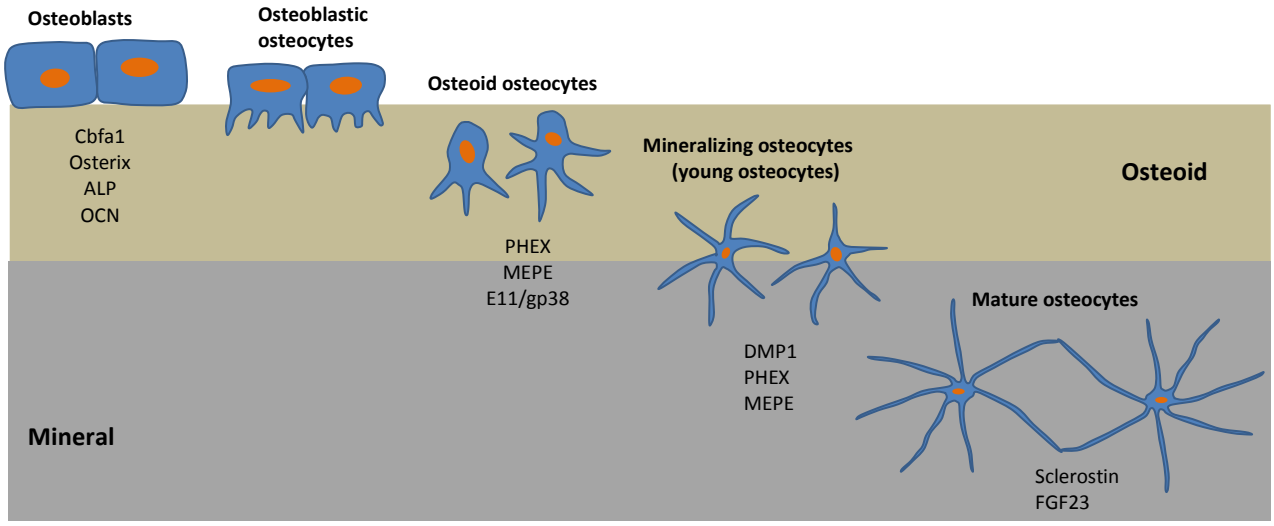

FIGURE 2. Schema describing the osteocyte differentiation process.

Mature osteoblasts express Cbfa1, Osterix, ALP and OCN. When they start to embed in the bone matrix, osteoblasts undergo a differentiation process toward osteoid osteocytes, mineralizing osteocytes and finally to mature osteocytes. E11/gp38 is one of the earliest specific proteins to be expressed during osteoblasts-to-osteocyte transition (osteoid osteocytes) [100]. DMP1 has high calcium ion-binding capacity [105], so it is expressed only in mineralized tissue [105,129]. DMP1 is a marker of transitioning osteocytes, and is expressed in young osteocytes. PHEX and MEPE regulate mineralization during osteocyte differentiation. MEPE is stimulated by Wnt3a and functions to inhibit bone mineralization by osteoblasts[130,131]. PHEX promotes bone mineralization. PHEX binds with high specificity to MEPE [132] to protect MEPE from proteolysis by cathepsin B[113]. Mature osteocytes express specific markers such as FGF23 which regulates phosphate homeostasis and sclerostin, which is an inhibitor of Wnt signaling and inhibits the proliferation and differentiation of osteoblasts [85].

ALP: Alkaline phosphatase; OCN: Osteocalcin; MEPE: Matrix extracellular phosphoglycoprotein; PHEX: Phosphate-regulating gene with homology to endopeptidases on the X chromosome; DMP1: Dentin matrix protein 1 and FGF23: Fibroblast growth factor 23.

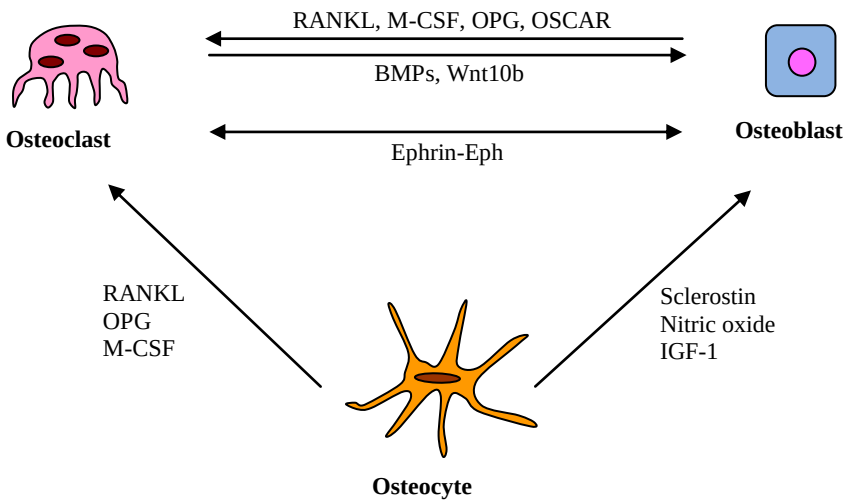

FIGURE 3. Signaling between bone cells.

Bone cells signal to each other via a number of cytokines and ligand-receptor interactions. Osteocytes secrete RANKL and M-CSF to activate osteoclast proliferation and differentiation, and this process is balanced by competitive binding of OPG to RANKL. IGF-1 from osteocytes induces osteoblast proliferation and differentiation. Nitric oxide activates osteoblast functions while sclerostin inhibits osteoblast functions. Osteoblasts also secrete RANKL, M-CSF, OPG as well as OSCAR, to regulate osteoclast proliferation and differentiation. Mature osteoclasts secrete BMPs and Wnt10b to activate osteoblast functions[133] and promote osteoblastogenesis[134] respectively. The ephrin (ligand)-EPH (receptor) complex is important for communication between osteoblasts and osteoclasts and regulates the activities of both cells, including regulating the differentiation of osteoblast lineage cells[135].

RANKL: Receptor activator of nuclear factor kappa-B ligand, M-CSF: macrophage colony-stimulating factor, OPG: Osteoprotegerin, OSCAR: *osteoclast*-associated receptor, BMP: bone morphogenetic protein, IGF: Insulin-like growth factor and Ephrin: Eph receptor interacting protein.

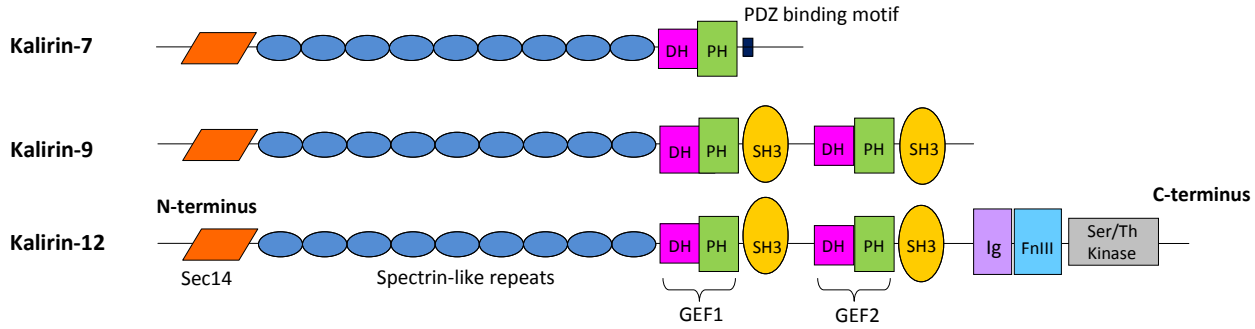

FIGURE 4. The domain structure of Kalirin isoforms.

Common domains of all three Kalirin major isoforms are Sec14, spectrin-like repeats and GEF1. Kalirin-9 is larger than Kalirin-7 with an additional GEF-2 domain. Kalirin-12 is the largest isoform with an additional GEF2, Ig, FnIII and Ser/Thr kinase domains.

DH: Dbl homology, PH: pleckstrin homology, GEF: guanine nucleotide exchange factor, SH3: Src homology domain, Ig: immunoglobulin-liked domain, FnIII: fibronectin III domain, and Ser/Thr: serine/threonine protein kinase domain.

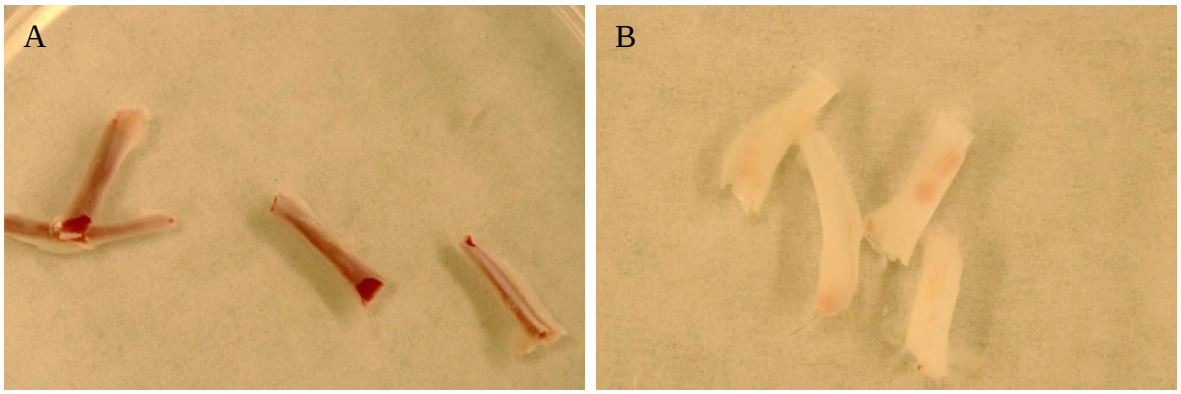

FIGURE 5. Mice tibias and femurs before and after bone marrow removal.

For osteocyte isolation, the bone marrow of tibias and femurs were flushed with sterilized PBS. Mice tibias and femurs before (A) and after (B) flushing with sterilized PBS are shown.

A.

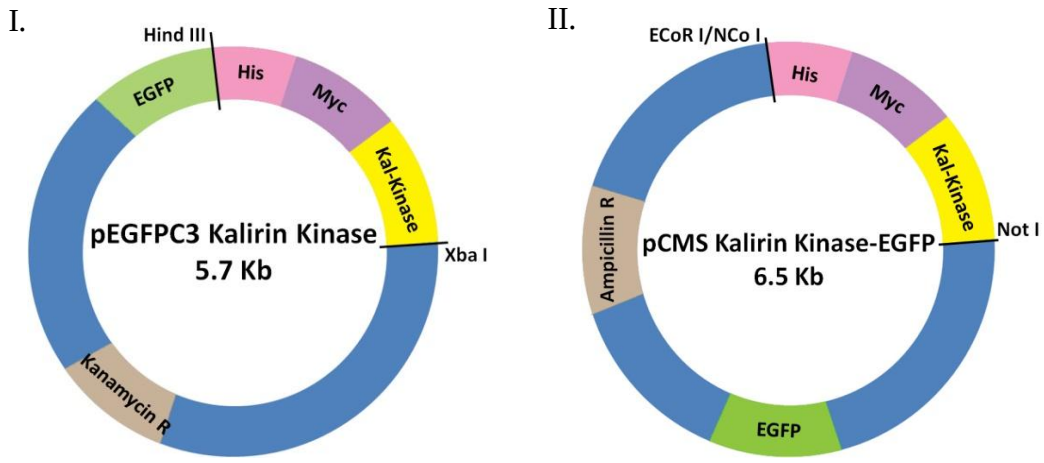

B.

Name	Vector	Insert	Size of insert	Total (kDa)
Kal-kinase1	pEGFP.Hismyc.Kal-kinase (GFP tagged)	EGFP Histidine Myc Kalirin Kinase	238 amino acids (26.9 kDa) 0.840 kDa 1.202 kDa 328 amino acid (36 kDa)	**65**
Kal-kinase2	pCMS.Hismyc.Kal-kinase (GFP co-expressed on a separate promoter)	Histidine Myc Kalirin Kinase	0.840 kDa 1.202 kDa 328 amino acid (36 kDa)	**38**
	pEGFP plasmid	GFP	238 amino acids	**26.9**

FIGURE 6. Domain structure of the Kalirin cDNA expression constructs.

(A) Schematic representation of the Kal-kinase1 (I) and Kal-kinase2 (II) cDNA expression plasmids are shown. Kalirin was tagged with histidine (His) and myc. (B) The predicted molecular weights of the protein domains are shown. The molecular weight of inserts is used to interpret Western blot assay results.

A.

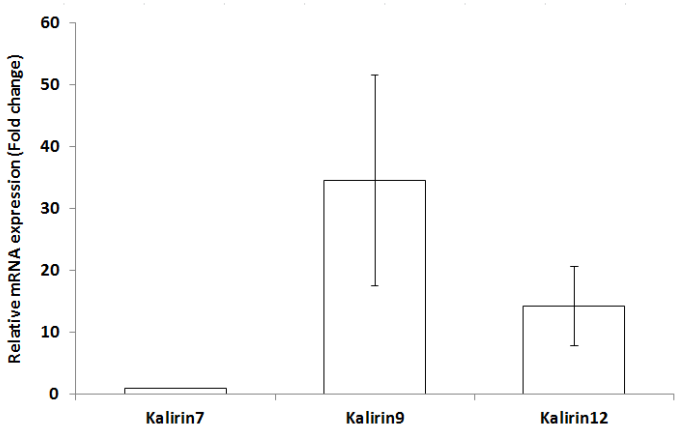

B.

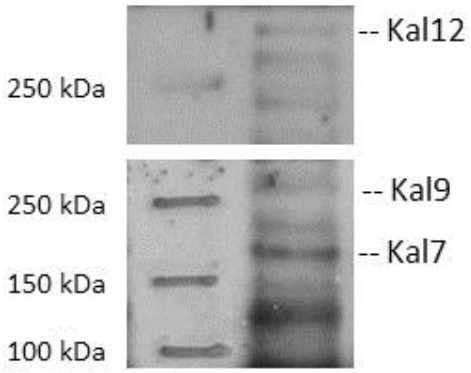

FIGURE 7. Determination of Kalirin mRNA and protein levels in osteocytes.

(A) The expression of Kalirin isoform mRNA levels in primary osteocytes (n=4) was quantified by QPCR. All three major isoforms are expressed. (B) The expression of Kalirin isoforms in MLO-Y4 cells was detected by Western blot analysis. Kalirin-7 was more highly expressed than Kalirin-9 at the protein level.

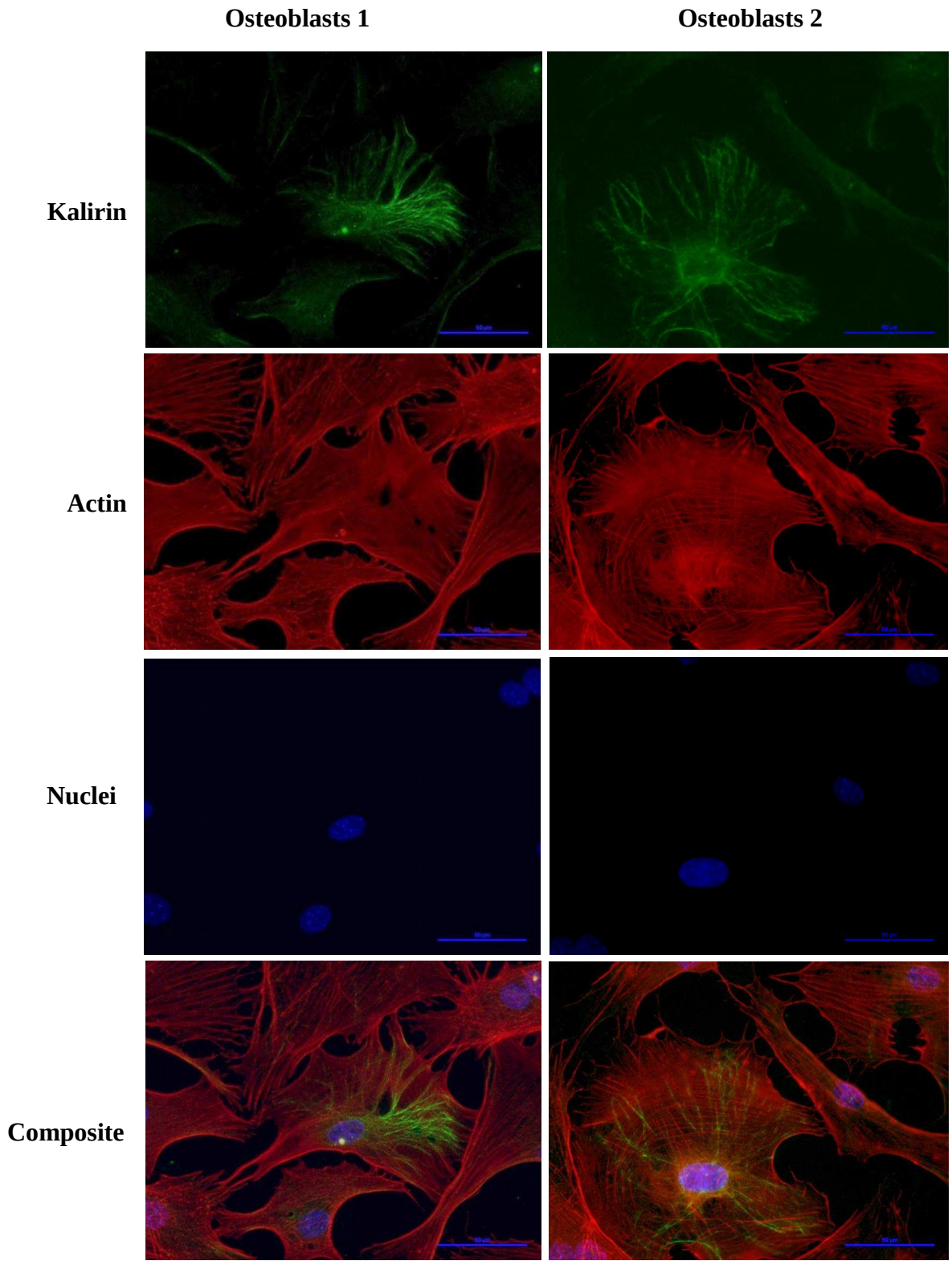

FIGURE 8. Immunofluorescent labeling of Kalirin in primary osteoblasts.

The immunofluorescent labeling of Kalirin (green), actin filaments (red), nuclei (blue) and composite of primary osteoblasts. The expression of Kalirin is at the perinuclear region and extending from the nucleus to the cell periphery.

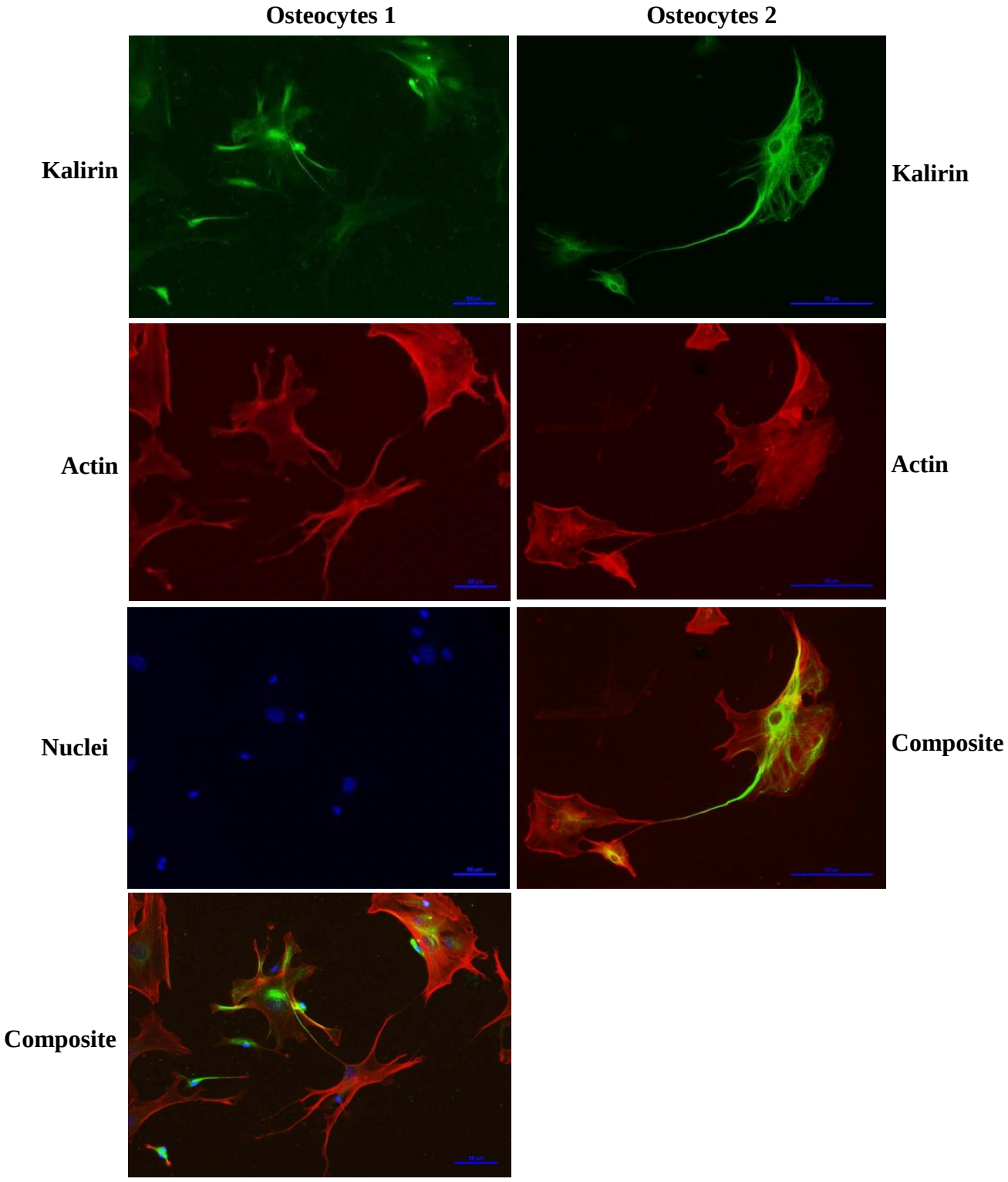

FIGURE 9. Immunofluorescent labeling of Kalirin in WT osteocytes.

The immunofluorescent labeling of Kalirin (green), actin filaments (red), nuclei (blue) and composite of WT osteocytes. Kalirin is localized to the perinuclear region and along the cytoplasmic processes, extending out to the tips of the processes of primary osteocytes.

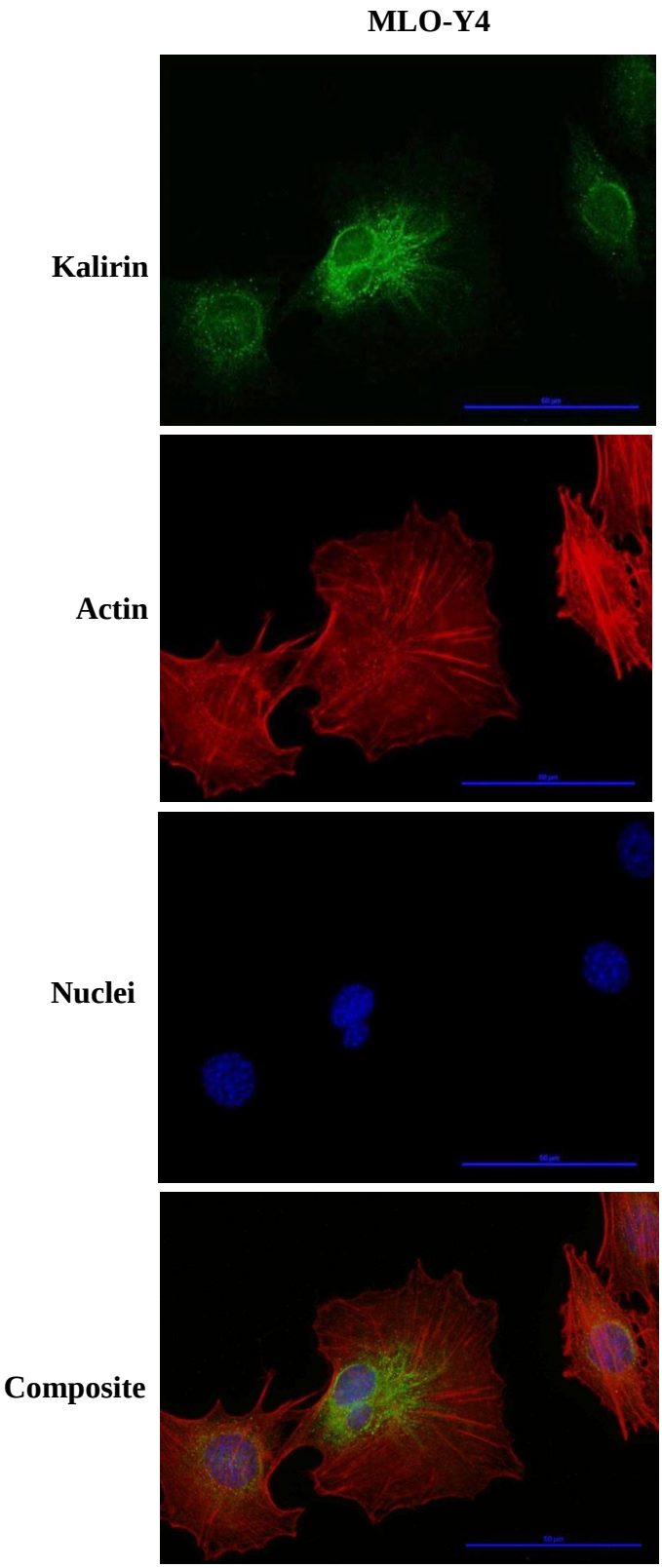

FIGURE 10. Immunofluorescent labeling of Kalirin in MLO-Y4 cells.

The immunofluorescent labeling of Kalirin (green), actin filaments (red), nuclei (blue) and composite of MLO-Y4 cells. Similar to primary osteocytes, Kalirin is localized to the perinuclear region in MLO-Y4 cells.

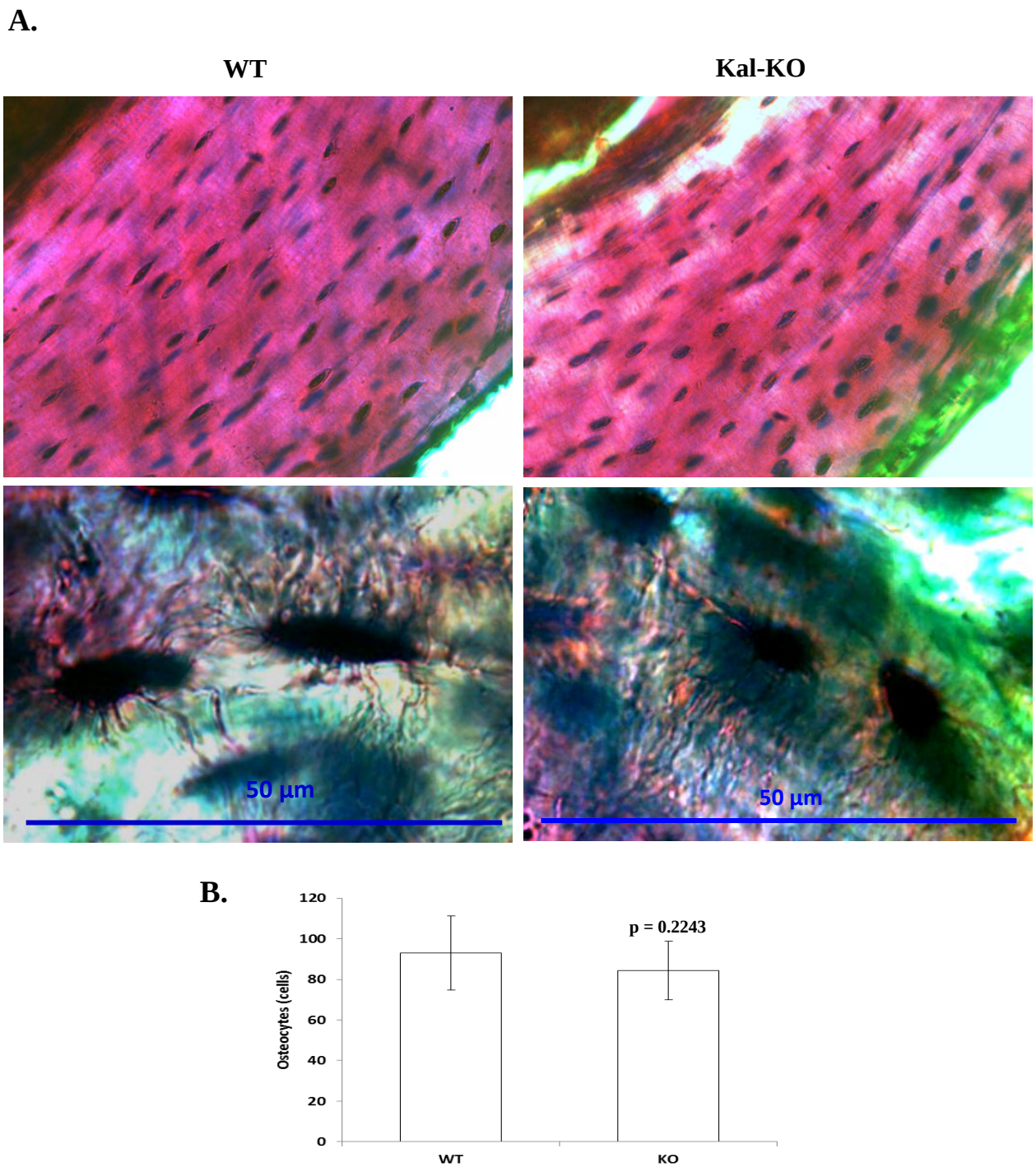

FIGURE 11. B**asic fuchsin staining of osteocytes in cortical bone.**

(A) Basic fuchsin stained osteocytes in lacuna in the cortical bones from the distal femurs of WT and Kal-KO mice. (B) Comparison of the number of osteocytes in tibias and femurs from WT and Kal-KO mice is shown. Statistical analysis was performed using mixed-model ANOVA (n=10). The number of osteocytes in cortical bone of WT and Kal-KO mice was not found to be statistically different ($p>0.05$).

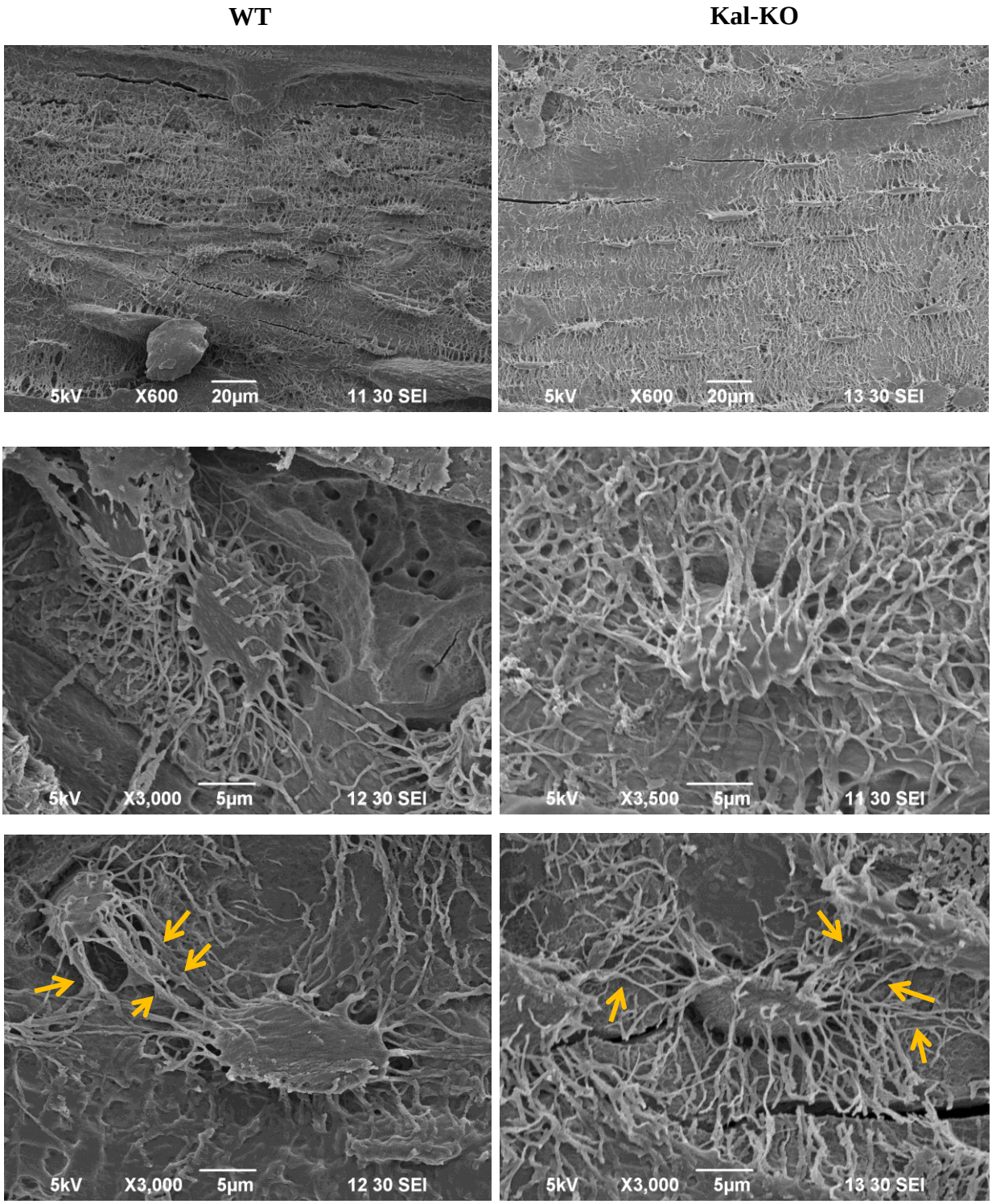

FIGURE 12. Analysis of osteocytes from Kal-KO and WT mice by SEM.

Representative SEM images after acid-etching of female long bones from Kal-KO and WT mice reveal osteocytes in lacuna. WT and Kal-KO osteocytes have numerous cytoplasmic processes extending from their cell bodies and joining the processes of adjacent cells (arrows).

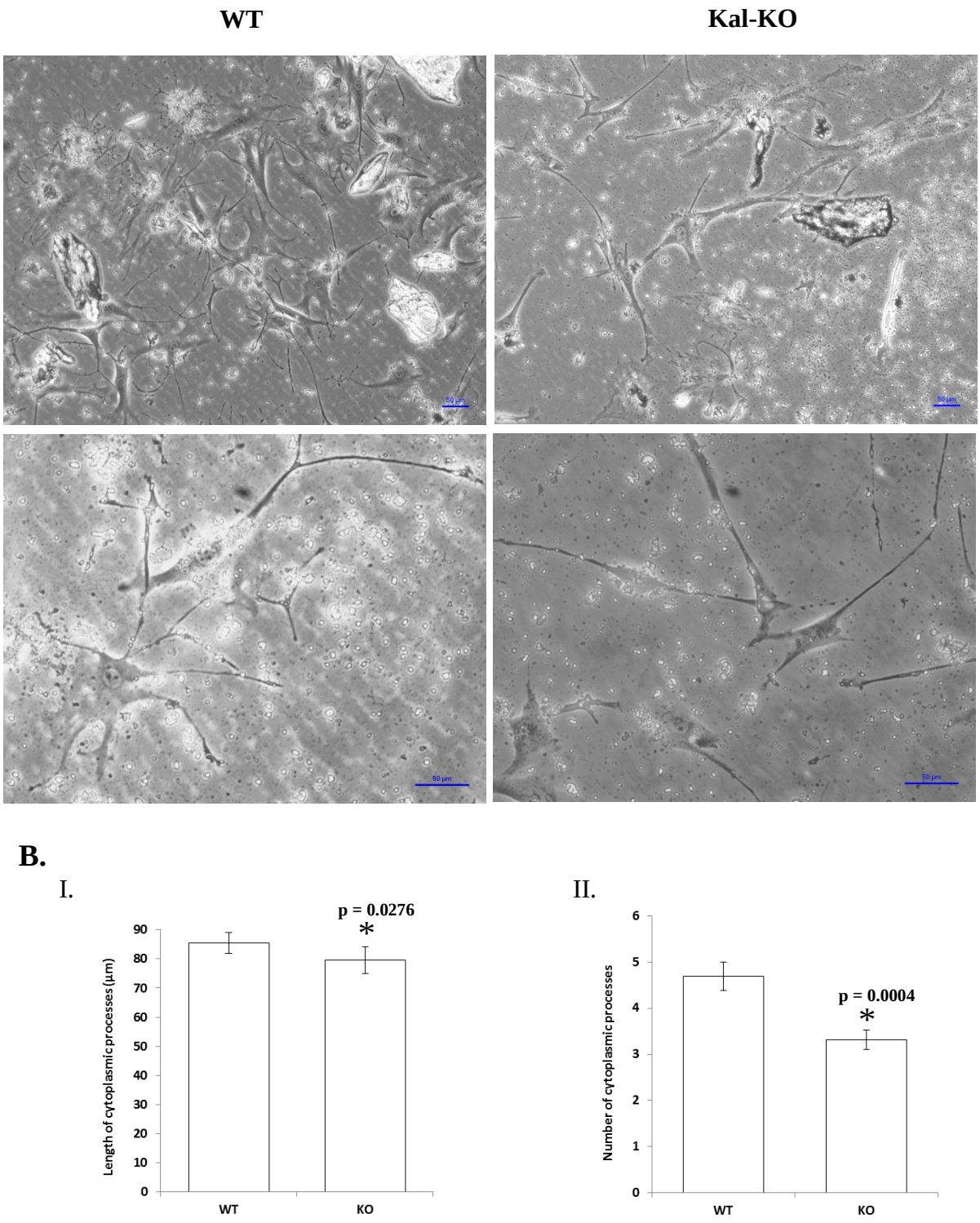

FIGURE 13. The morphology of primary osteocytes from WT and Kal-KO mice.

(A) A morphology of osteocytes from the tibias and femurs of WT and Kal-KO mice (n=8 and 7, respectively) cultured on collagen-coated plates for one month after isolation. (B) The average length and number of cytoplasmic processes per cell in WT and Kal-KO osteocyte (n=68 and 78 cells, respectively) is shown. Kal-KO osteocytes have significantly shorter and fewer processes than the WT group ($p<0.05$ base on the Wilcoxon rank sum test).

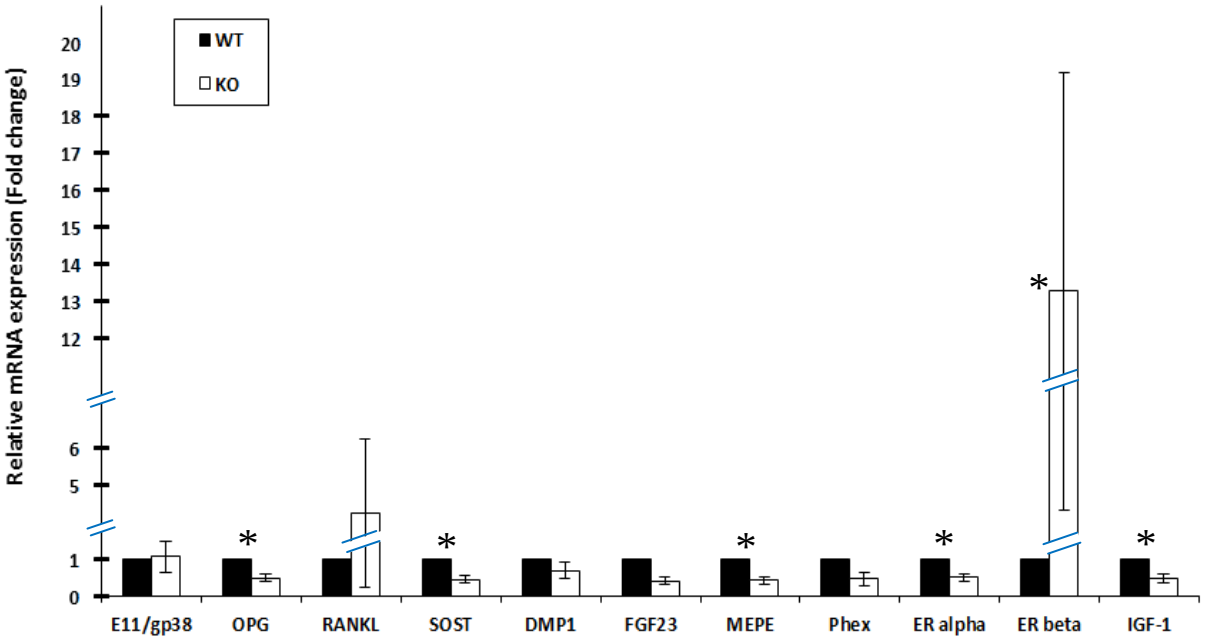

Detector	Mean±SE	p-value
E11/gp38	1.07±0.42	0.84
OPG	0.50±0.09	0.0313
RANKL	4.25±2.01	0.11
SOST	0.45±0.1	0.0156
DMP1	0.70±0.21	0.31
FGF23	0.73±0.32	0.63
MEPE	0.43±0.1	0.0313
Phex	0.46±0.17	0.08
ER alpha	0.51±0.1	0.0156
ER beta	13.26±7.94	0.0313
IGF-1	0.49±0.13	0.0313

FIGURE 14. Comparison of mRNA expression levels in WT and Kal-KO osteocytes.

The expression of specific osteocyte genes detected in WT and Kal-KO osteocytes was quantified by QPCR, normalized to *18S* RNA and compared. The experiment was repeated 4 times and results from all experiments were averaged. Asterisks in the graph and highlighted p-values in a table show the statistic difference between WT and Kal-KO osteocyte genes.

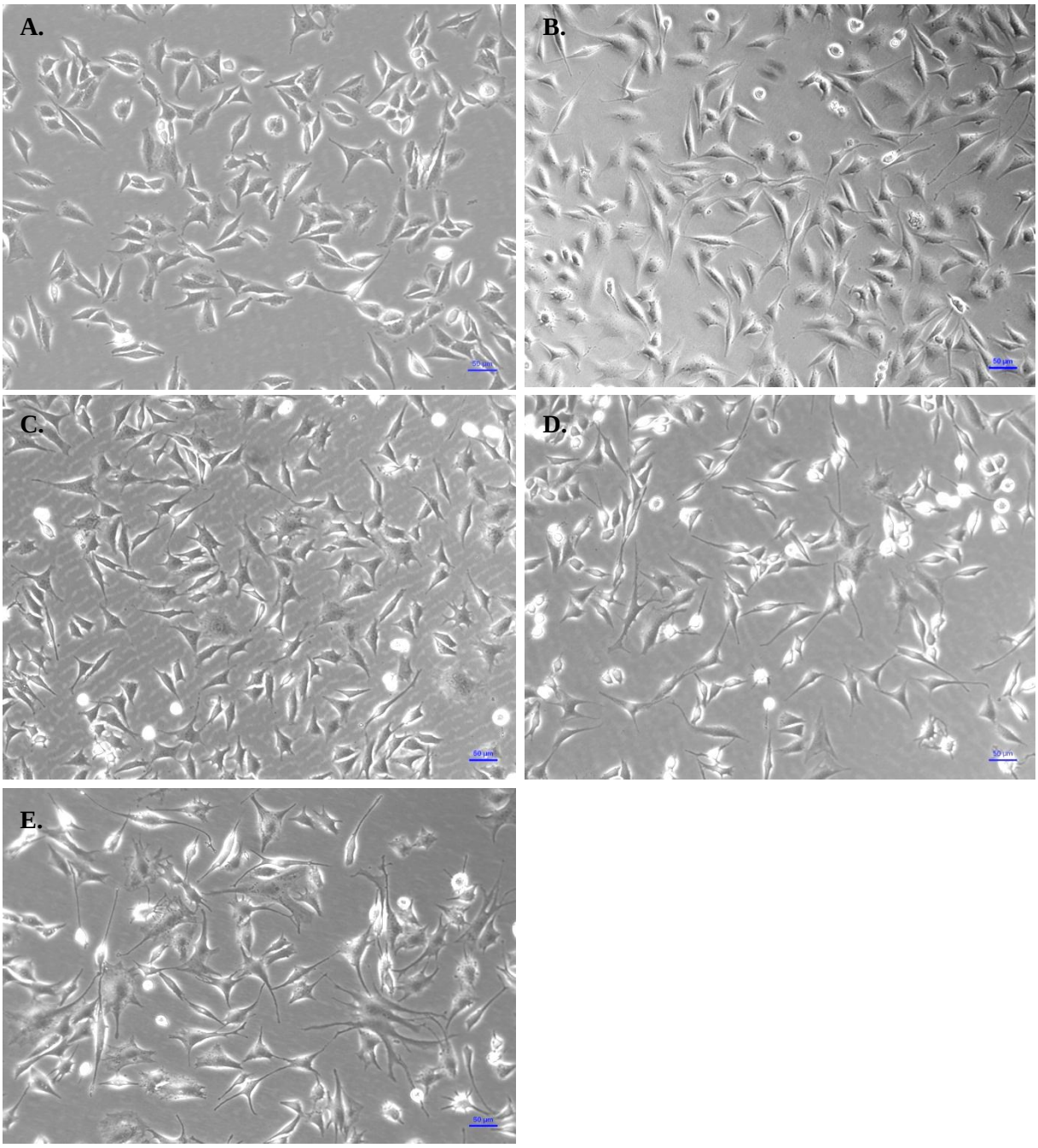

FIGURE 15. The morphology of MLO-Y4 cells after treatment with NGF or KCl.

Representative images of the morphology of untreated MLO-Y4 cells compared with cells treated with increasing concentrations of nerve growth factor (NGF-β) or KCl for 5 days. (A, control; B, 25ng/ml NGF; C, 50 ng/ml NGF; D, 75 ng/ml NGF; E, 50 mM KCl). MLO-Y4 cells treated with high concentrations of NGF or KCl exhibit a distinct elongation of their cytoplasmic processes compared to untreated control cells. Experiments were reproduced 4 times.

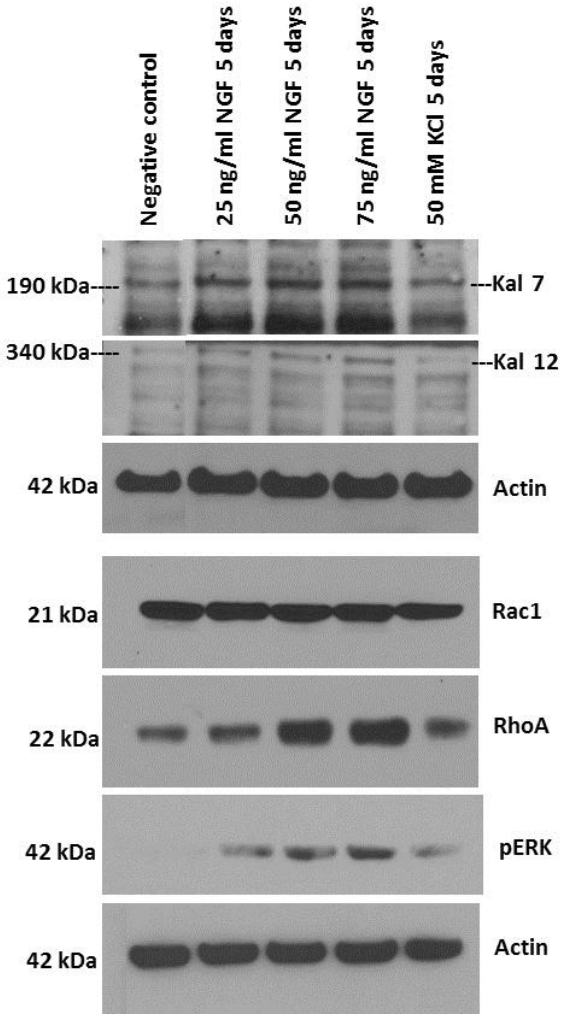

FIGURE 16. Western blot analysis of MLO-Y4 cells treated with NGF or KCl.

Western blot analysis of Kalirin-7, Kalirin-12, RhoA and pERK from total cell lysate of MLO-Y4 treated with increasing concentration of NGF or KCl. The highest expression of Kalirin-7, Kalirin-12, RhoA and pERK were observed in the 75 ng/ml NGF treatment group in which cytoplasmic processes were elongated (see Figure 13).

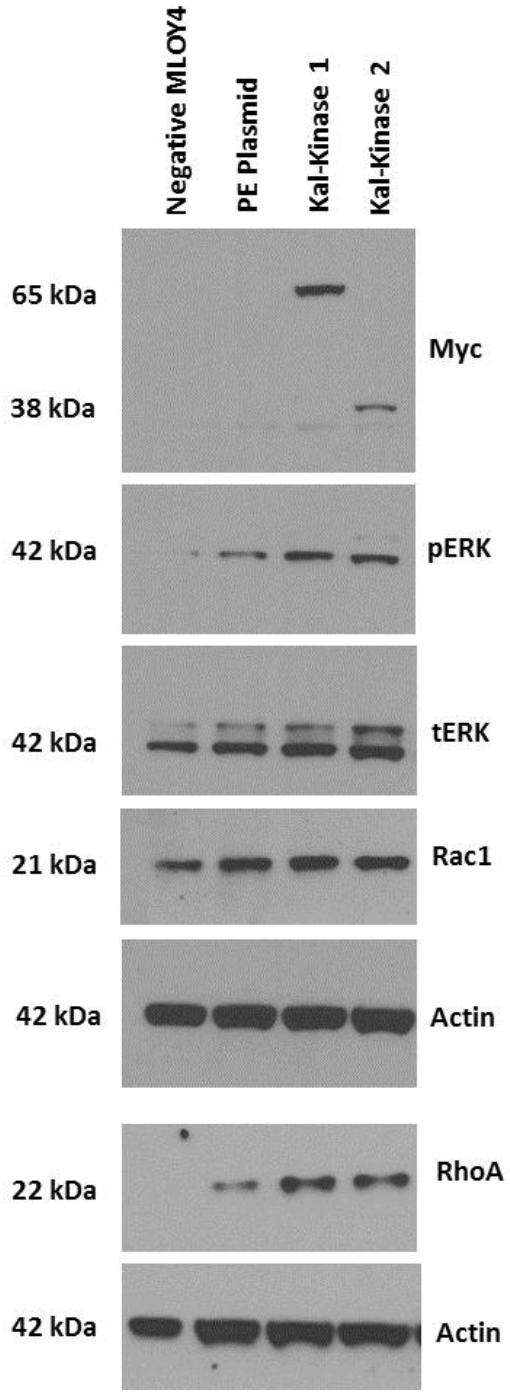

FIGURE 17. Western blot analysis of MLO-Y4 cells expressing the Kalirin-12 kinase domain.

The Kalirin-12 kinase domain was expressed in MLO-Y4 cells by electroporation. The expression constructs for the Kalirin-12 kinase domain each contained a myc tag which was detected with an anti-myc antibody by Western blot assay. The myc blot represents the expression level of the kinase domain after electroporation. Controls included non-electroporated cells and cells electorporated with a PE plasmid (empty plasmid). The expression of pERK and RhoA in Kal-kinase domain expressing cells were higher than the negative control groups.

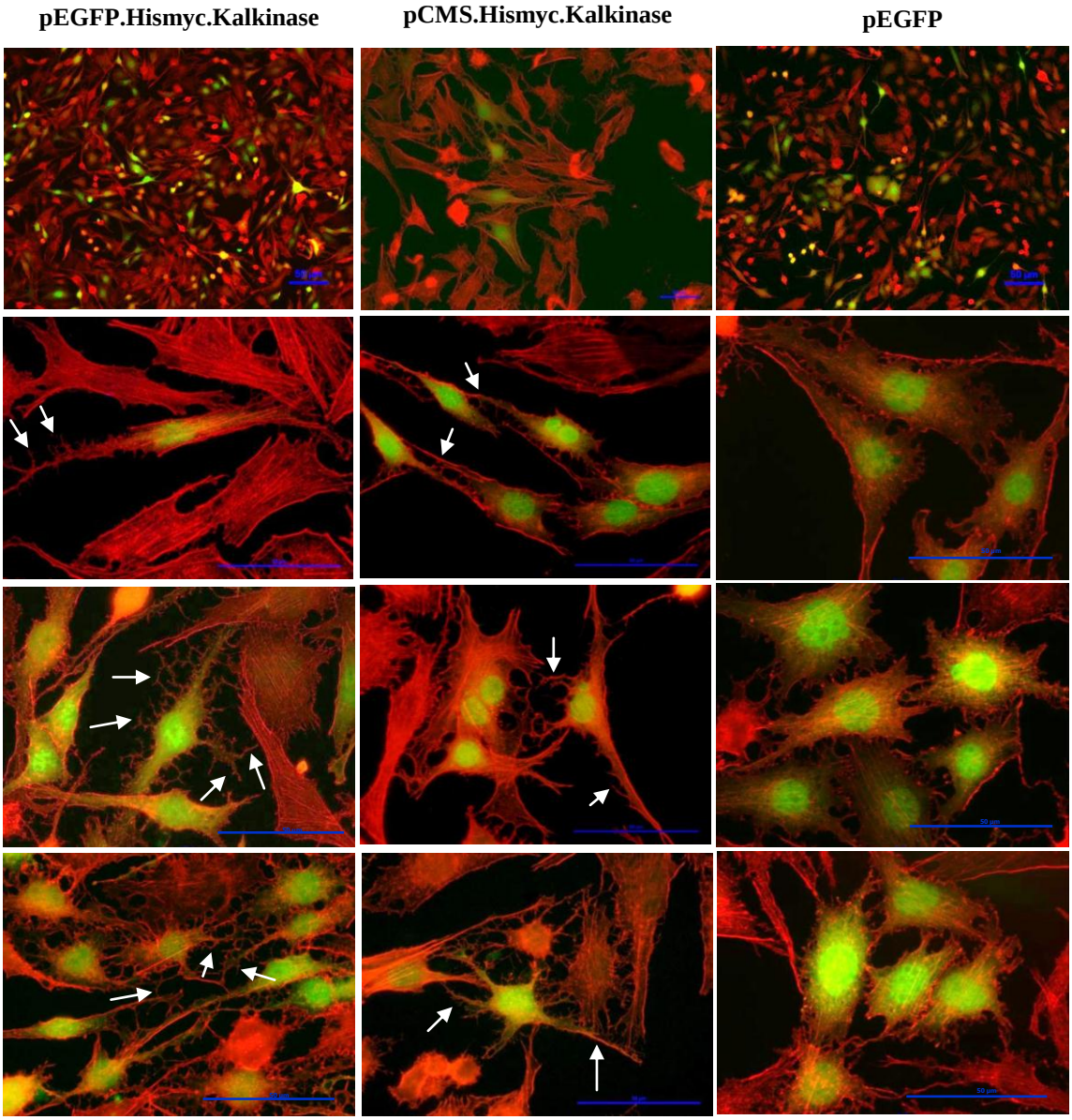

FIGURE 18. Immunofluorescent labeling of MLO-Y4 cells expressing the Kalirin-12 kinase domain.

Kalirin Ser-Thr kinase domain plasmids (pEGFP.Hismyc.Kalkinase and pCMS.Hismyc.Kalkinase) tagged with GFP were transfected into MLO-Y4 cells by electroporation. The control group was transfected with empty pGFP plasmid, expressing GFP. Transfected MLO-Y4 cells were detected by virtue of GFP (green) while the actin cytoskeleton was detected by staining with rhodamine phalloidin (red). Cells expressing the Ser-Thr kinase domain (green cells) exhibit more branching of their cytoplasmic processes compared with non-transfected cells (not expressing GFP).

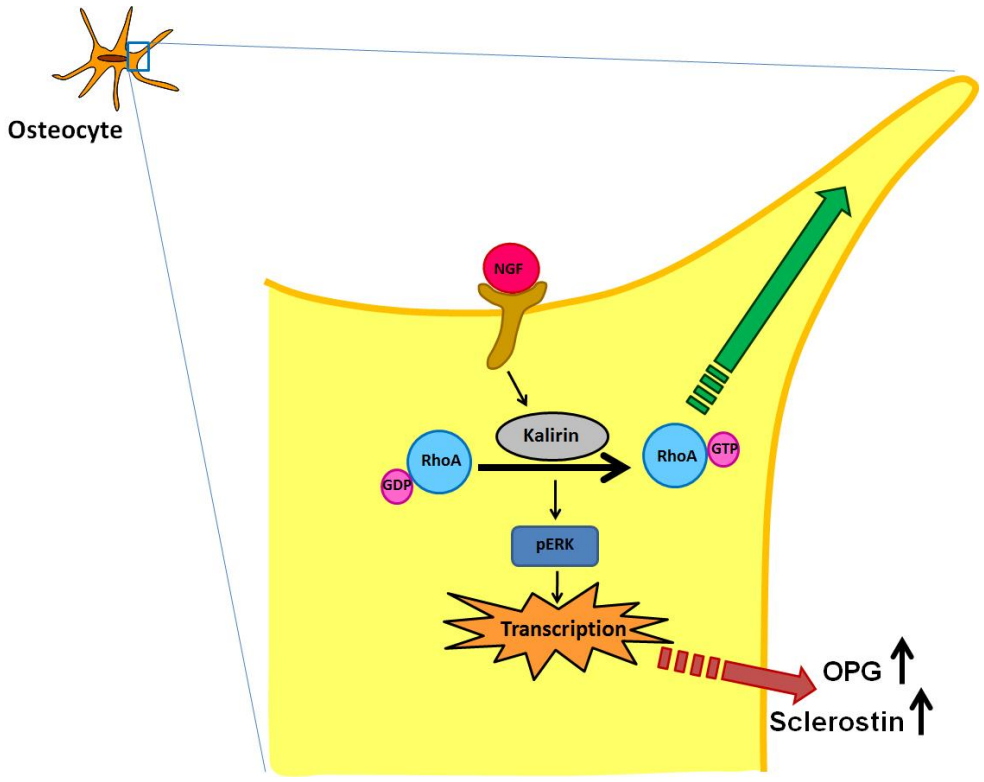

FIGURE 19. Working model for the mechanism of action of Kalirin in osteocytes.

In wild-type osteocytes, external stimuli such as nerve growth factor activates Kalirin. Activated Kalirin promotes RhoA-GTP binding, resulting in the reorganization of actin cytoskeleton and the elongation of the cytoplasmic processes in osteocytes. In addition, the Ser-Thr kinase of Kalirin potentially leads to the phosphorylation of ERK, which in turn may lead to *OPG* and *SOST* transcription. In the absence of Kalirin, changes in the length of osteocyte dendritic spines as well as decreased secretion of OPG and sclerostin may potentially regulate osteocyte communication, osteoclast differentiation and osteoblast activity, respectively.

DISCUSSION

Osteocytes are deeply embedded within the mineralized bone matrix, making their biology difficult to examine. As a result, much less is known about this cell type than osteoblasts, from which they are differentiated. In 2010, Kramer *et al*. reported that genetically modified mice lacking β-catenin only in osteocytes (driven by the DMP1-Cre promoter), exhibited progressive bone loss, growth retardation and premature lethality. Cancellous bone mass was almost completely absent and cortical bone thickness was severely reduced [136]. In other studies, it was shown that the cytoplasmic processes of osteocytes are very important for osteocyte viability and their ability to communicate with each other as well as osteoblasts and osteoclasts [137]. In addition, osteocytic processes regulate the cell's ability to respond to mechanical stimuli, fluid shear stress and changes in circulating levels of hormones, calcium or phosphate. However, a clear mechanistic understanding of the extension/retraction of the osteocyte cytoplasmic processes and their role in bone homeostasis is lacking.

Most studies to date have focused on the role of the novel GEF protein, Kalirin, in brain tissue and neuronal plasticity. Kalirin-7 mRNA was the most abundant isoform found in neurons of the central nervous system [58]. Kalirin-9 and Kalirin-12 were found to be highly expressed during embryonic development, with Kalirin-7 protein levels increasing in adult brain [58]. In the current study, the influence of Kalirin on the function of osteocytes and the formation of cytoplasmic processes in osteocytes was examined. QPCR analysis of Kalirin isoforms in primary osteocytes and MLO-Y4 osteocytic cells revealed that Kalirin-9 mRNA was more abundant than Kalirin-12, followed by Kalirin-7 mRNA. On the other hand, Western blot analysis indicated that Kalirin-7 was more highly expressed than Kalirin-9 and Kalirin-12. However, the latter finding may be due to differences in the specificity of the polyclonal antibodies used in these studies. Alternatively, it is possible that the isoforms exhibit differences in mRNA or protein stability. Further study is needed to clarify the expression and functions of the three major Kalirin isoforms in osteocytes.

To examine the effects of Kalirin on the number of osteocytes, basic fuchsin staining of mouse distal femurs was used, which revealed a similar numbers of osteocytes in Kal-KO and WT cortical bones. To quantify differences in osteocyte cytoplasmic extensions, primary osteocytes were isolated and examined

in vitro using phase-contrast and immunofluorescent microscopy. The morphology of osteoblasts and osteocytes was found to be distinctly different, especially with the appearance of cytoplasmic processes in osteocytes. Primary osteocytes from WT mice contained an average of 4.7±0.3 cytoplasmic extensions per cell, which were 85±3.6 μm in length. In contrast, the number (3.3±0.2) and length (79.5±4.6 μm) of cytoplasmic extensions in primary osteocytes from Kal-KO mice were significantly reduced. In 2005, Holmbeck *et al*. used Bodian silver stain to directly observe the length and number of processes of osteocytes in bone pieces from tibia and femur of WT mice. Cytoplasmic processes were found to be 4-8 μm in length, and 9-26 cytoplasmic processes per osteocyte were reported [29]. In 2006, Beno *et al*. reported 40-100 cytoplasmic processes per osteocyte [138]. Thus, the number of osteocyte cytoplasmic processes reported in bone sections appears to be significantly higher than the number of processes identified in our studies using primary osteocytes cultured *in vitro.* The discrepancy in these findings may be due to the fact that the length of cytoplasmic processes in bone may be constrained by the mineralized matrix and the established canaliculi network, and by the number of neighboring osteocytes or other bone cells. In vitro, however, these physical constraints may be eliminated or reduced allowing for lengthening of cytoplasmic processes. The number and length of cytoplasmic processes may also be affected by plating density. Indeed, collagenase digestion of bone yields a small number of osteocytes, which when cultured are physically isolated from other osteocytes. As osteocytes re-establish a communication network, the lengthening of individual cytoplasmic processes may be favored rather than altering the number of processes per cell. Immunofluorescent staining also revealed the perinuclear localization of Kalirin in primary osteocytes (Figure 9) and MLO-Y4 cells (Figure 10). Kalirin also colocalized with a subset of radially-directed actin filaments which extended outwards towards the plasma membrane. Taken together, our studies demonstrate that Kalirin plays a role in regulating both the length and number of cytoplasmic extensions in primary osteocytes. Future studies will examine the effect of cell density on the length and number of cytoplasmic processes in primary osteocytes from WT and Kal-KO mice.

After serial collagenase digestion of bones to isolate primary osteocytes, deeply embedded osteocytes remaining in bones were examined for changes in mRNA expression. Several genes specific for osteoblasts or osteocytes were examined from these bones. mRNA for *SOST, DMP1* and *E11/gp38* were

all detected. In contrast, the expression of KERA, which is the specific marker for osteoblasts not detected (data not shown). Therefore, mature osteocytes were the main cellular source or RNA present in these bones.

To examine the role of Kalirin on osteocyte function, QPCR analysis of osteocyte genes was performed. Several osteocyte markers were examined including markers for early osteoid osteocytes (*MEPE*, *PHEX* and *E11/gp38*), mineralized osteocytes (*Dmp1*) and mature osteocytes (*FGF23* and *SOST*) [139]. E11/gp38 is the earliest osteocyte-specific protein (osteoid osteocytes), which is expressed early during the transition of osteoblasts to osteocytes [100]. Although no change in the level of *E11/gp38* was detected in Kal-KO osteocytes, potentially indication a similar number of osteocytes were present in these bone preparations, a significant decrease in *MEPE* mRNA was observed in Kal-KO osteocytes, compared to WT cells, suggesting that Kalirin may play a role in the mineralizing activity of osteocytes. QPCR analysis also revealed a decrease in *SOST* mRNA levels, suggesting that sclerostin secretion by Kal-KO osteocytes may be decreased. Since sclerostin is involved in antagonizing Wnt signaling in osteoblasts, resulting in an increase in β-catenin degradation [140,141]. These findings suggest that osteocyte-osteoblast communication may be impaired in the absence of osteocytic Kalirin. The decrease in sclerostin mRNA suggested that osteoblast activity may be enhanced. Consistent with this finding, unpublished findings from this laboratory suggest that the differentiation of early osteoblasts is enhanced in Kal-KO osteoblasts. However, Kal-KO osteoblasts also exhibit a decrease in the mineralizing activity of mature osteoblasts, which may contribute to the decrease in cortical bone mass observed in Kal-KO female mice (Huang *et al*. unpublished data).

The estrogen receptors (ERs) are nuclear hormone receptors which can initiate or enhance gene transcription [142]. Osteocytes in cortical bone strongly express ER-α while osteocytes in trabecular bone predominately express ER-β [120]. Moreover, low levels of estrogen or defects in estrogen signaling leads to bone loss, in part by promoting osteoclast survival [143]. QPCR analysis revealed a decrease in *ER-α* and an increase in *ER-β* in Kal-KO compared to WT osteocytes. The osteocyte preparations for this study consisted of pooled cells from cortical and trabecular bone. The decrease of *ER-α* and increase in *ER-β*

mRNA levels may therefore indicate that estrogen-signaling is disrupted in Kal-KO mice, potentially contributing to the reduced bone mass of female Kal-KO mice. Consistent with this speculation, osteoclast number was increased in femoral sections of Kal-KO mice (Huang *et al*., unpublished studies). Osteoclast differentiation is also controlled by the ratio of RANKL and OPG, which acts as a decoy receptor for RANKL. QPCR analysis revealed a decrease in OPG mRNA levels in Kal-KO osteocytes, which could lead to alterations in the RANKL/OPG ratio and further promote osteoclast differentiation.

Osteocytes express a large amount of IGF-1, which acts as an osteogenic growth factor to promote bone formation by osteoblasts [144]. *IGF-1* mRNA is also upregulated in osteocytes in response to mechanical loading [145]. In transgenic mice in which IGF-1 over-expression was targeted to osteoblasts using the osteocalcin promoter, an increase in bone mineral density and bone volume was observed [146]. In addition, an increase in osteocyte lacunae occupancy was observed, suggesting that IGF-I may extend osteocyte life span. In osteocytes from Kal-KO mice, a decrease in *IGF-1* mRNA levels was observed by QPCR, suggesting that osteocyte life-span may be decreased in Kal-KO mice compared to WT osteocytes. Kal-KO mice may also be less responsive to mechanical loading. However, the physiological consequence of reduced *IGF-1* mRNA levels in Kal-KO osteocytes remains to be determined.

Overall, QPCR analysis of osteocytes from WT and Kal-KO mice suggest defects in the function of osteocytes as well as their ability to regulate the activities of osteoblasts and osteoclasts. However, at this time, we cannot exclude the possibility that sequential collagenase digestions from WT and Kal-KO bones (which are osteoporotic) did not lead to the isolation of a different subset of osteocytes from the different mice genotypes. Future studies will include comparing the expression of osteocyte mRNA levels in collagenase and non-collagenase treated bones as well as from isolated osteocytes.

To study the mechanism of Kalirin's effects on cytoplasmic elongation in osteocytes, the functional domains of Kalirin were introduced into MLO-Y4 cells by electroporation. The cytoplasmic processes of MLO-Y4 cells over-expressing the Ser-Thr kinase domain of Kalirin-12 were found to be longer and more branched than control cells. Furthermore, an increase in the expression of phosphorylated ERK was

observed in cells expressing the Ser-Thr kinase domain. Of interest, mechanical stimulation promotes the survival of osteocytes by activating ERK signaling [147]. Moreover, Plotkin *et al*. reported that ERK signaling was not activated by mechanical loading in ER-α and ER-β knock-down osteocytes [148]. Based on these findings, it is possible that Kalirin may be involved in promoting cytoplasmic spine elongation in osteocytes via an ER- and/or ERK-dependent pathway following mechanical stimulation.

High extracellular KCl has been shown to promote the elongation of cytoplasmic processes in neurons, which is dependent on chloride channel activation [88]. Chakrabarti *et al*. also reported that Kalirin bound to the NGF receptor TrkA in neurons and induced the extension of dendritic processes of neurons[87]. Therefore, we speculated that osteocyte dendritic processes might be regulated by NGF or KCL. Interestingly, the cytoplasmic processes of MLO-Y4 cells were found to be dose-dependently increased in the presence of NGF. KCl-treated MLO-Y4 cells also showed significant elongation of their cytoplasmic processes compared to control cells. Western blot analysis further revealed that NGF dose-dependently increased the protein levels of Kalirin-7, Kalirin-12 and RhoA in MLO-Y4 cells. Although KCl-treated cells exhibited elongated cytoplasmic processes, the expression of Kalirin-7, Kalirin-12 and RhoA were lower than in the NGF-treated cells, suggesting that KCl promoted the elongation of cytoplasmic processes via a different intracellular mechanism than NGF. Furthermore, the ability of NGF to promote cytoplasmic process elongation appeared to involve Kalirin and RhoA, which is a known Kalirin GEF target. Future studies will focus on understanding the mechanism of action of NGF and KCL on dendritic spine elongation in osteocytes, and on identifying the NGF receptors expressed in osteocytes, which currently remain unknown.

SUMMARY AND CONCLUSIONS

Osteocytes are deeply embedded within the mineralized matrix, and play an essential role in the regulation of bone mass via cellular communication with osteoclasts and osteoblasts. Kalirin was found to be expressed in osteoclasts and osteoblasts and global deletion of Kalirin leads to a loss of trabecular and cortical bone mass. We examined the role of Kalirin on the morphology and function of osteocytes. Quantitative PCR (QPCR) and Western blotting revealed the expression of the three major Kalirin isoforms (Kal-7, Kal-9, Kal-12) in osteocytes, while immunofluorescent staining revealed Kalirin was localized to the perinuclear region and the cytoplasmic processes of osteocytes. In the absence of Kalirin, the number and length of cytoplasmic processes were significantly reduced in osteocytes, suggesting Kalirin regulates cytoskeletal remodeling. Moreover, the mRNA levels of osteoprotegerin and SOST, which are important for controlling osteoclast differentiation and Wnt signaling leading to bone formation by osteoblasts, respectively, were reduced in Kal-KO osteocytes. Finally, MLO-Y4 cells treated with NGF, which is known to activate Kalirin in neurons, or over-expressing the Ser-Thr kinase domain of Kal-12, promoted cytoplasmic process elongation and upregulated phosphorylated ERK and RhoA levels.

Overall, these results suggest that Kalirin controls osteocyte morphology and function in part by regulating cytoskeletal remodeling and the activity of ERK and RhoA. Kalirin is also involved in intercellular signaling via sclerostin and OPG to regulate both osteoblast function and osteoclast differentiation, respectively. Furthermore, Kalirin may regulate the bone remodeling process *in vivo* through direct and indirect effects on the function of osteoclasts, osteoblasts and osteocytes.

REFERENCES

1. Riancho JA, HernÃ¡ndez JL. Pharmacogenomics of osteoporosis: a pathway approach. Pharmacogenomics 2012;13(7):815-829.
2. Murray P, Huxley J. Self-Differentiation in the Grafted Limb-Bud of the Chick. J Anat 1925;59:379-384.
3. Soltanoff C, Yang S, Chen W, Li Y. Signaling networks that control the lineage commitment and differentiation of bone cells. Crit Rev Eukaryot Gene Expr 2009;19(1):1-46.
4. Orwoll ES. Toward an Expanded Understanding of the Role of the Periosteum in Skeletal Health. Journal of Bone and Mineral Research 2003;18(6):949-954.
5. Einhorn T. The cell and molecular biology of fracture healing. Clin Orthop Relat Res 1998:7-21.
6. Xiong J, O'Brien CA. Osteocyte RANKL: New insights into the control of bone remodeling. Journal of Bone and Mineral Research 2012;27(3):499-505.
7. Organization WH. WHO scientific group on the assessment of osteoporosis at primary health care level. Brussels, Belgium: World Helath organization; 2004 5-7 May 2004.
8. Bellido T, Plotkin LI. Novel actions of bisphosphonates in bone: Preservation of osteoblast and osteocyte viability. Bone 2011;49(1):50-55.
9. Pineda B, Hermenegildo C, Tarín J, Cano A, García-Pérez M. Effects of administration of hormone therapy or raloxifene on the immune system and on biochemical markers of bone remodeling. Menopause 2012;19(3):319-327.
10. Das S, Crockett J. Osteoporosis - a current view of pharmacological prevention and treatment. Drug Des Devel Ther 2013;31(7):435-448.
11. Fromigué O, Haÿ E, Barbara A, Petrel C, Traiffort E, Ruat M, Marie PJ. Calcium sensing receptor-dependent and receptor-independent activation of osteoblast replication and survival by strontium ranelate. Journal of Cellular and Molecular Medicine 2009;13(8b):2189-2199.
12. Yang F, Yang D, Tu J, Zheng Q, Cai L, Wang L. Strontium Enhances Osteogenic Differentiation of Mesenchymal Stem Cells and In Vivo Bone Formation by Activating Wnt/Catenin Signaling. Stem Cells 2011;29(6):981-991.
13. Jilka R, Weinstein R, Bellido T, Roberson P, Parfitt A, Manolagas S. Increased bone formation by prevention of osteoblast apoptosis with parathyroid hormone. J Clin Invest 1999;104(4):439-446.
14. Stern AR, Nicolella DP. Measurement and estimation of osteocyte mechanical strain. Bone 2013;54(2):191-195.
15. Nakashima T, Hayashi M, Fukunaga T, Kurata K, Oh-hora M, Feng JQ, Bonewald LF, Kodama T, Wutz A, Wagner EF and others. Evidence for osteocyte regulation of bone homeostasis through RANKL expression. Nat Med 2011;17(10):1231-1234.
16. Boyle WJ, Simonet WS, Lacey DL. Osteoclast differentiation and activation. Nature 2003;423(6937):337-342.
17. Zhao S, Kato Y, Zhang Y, Harris S, Ahuja SS, Bonewald LF. MLO-Y4 Osteocyte-Like Cells Support Osteoclast Formation and Activation. Journal of Bone and Mineral Research 2002;17(11):2068-2079.

18. Harada S-i, Rodan GA. Control of osteoblast function and regulation of bone mass. Nature 2003;423(6937):349-355.
19. Day TF, Guo X, Garrett-Beal L, Yang Y. Wnt/β-Catenin Signaling in Mesenchymal Progenitors Controls Osteoblast and Chondrocyte Differentiation during Vertebrate Skeletogenesis. Developmental Cell 2005;8(5):739-750.
20. Matsuo K. Cross-talk among bone cells. Curr Opin Nephrol Hypertens 2009;18(4):292-297.
21. Edwards C, Mundy G. Eph receptors and ephrin signaling pathways: a role in bone homeostasis. Int J Med Sci 2008;5(5):263-272.
22. Kamioka H, Sugawara Y, Honjo T, Yamashiro T, Takano-Yamamoto T. Terminal Differentiation of Osteoblasts to Osteocytes Is Accompanied by Dramatic Changes in the Distribution of Actin-Binding Proteins. Journal of Bone and Mineral Research 2004;19(3):471-478.
23. Paznekas WA, Boyadjiev SA, Shapiro RE, Daniels O, Wollnik B, Keegan CE, Innis JW, Dinulos MB, Christian C, Hannibal MC and others. Connexin 43 (GJA1) Mutations Cause the Pleiotropic Phenotype of Oculodentodigital Dysplasia. The American Journal of Human Genetics 2003;72(2):408-418.
24. Zhu J, Sasano Y, Takahashi I, Mizoguchi I, Kagayama M. Temporal and spatial gene expression of major bone extracellular matrix molecules during embryonic mandibular osteogenesis in rats. Histochem J 2001;33(1):25-35.
25. You L-D, Weinbaum S, Cowin SC, Schaffler MB. Ultrastructure of the osteocyte process and its pericellular matrix. The Anatomical Record Part A: Discoveries in Molecular, Cellular, and Evolutionary Biology 2004;278A(2):505-513.
26. Knothe Tate ML, Niederer P, Knothe U. In Vivo Tracer Transport Through the Lacunocanalicular System of Rat Bone in an Environment Devoid of Mechanical Loading. Bone 1998;22(2):107-117.
27. Ohuchi E, Imai K, Fujii Y, Sato H, Seiki M, Okada Y. Membrane Type 1 Matrix Metalloproteinase Digests Interstitial Collagens and Other Extracellular Matrix Macromolecules. Journal of Biological Chemistry 1997;272(4):2446-2451.
28. Koshikawa N, Giannelli G, Cirulli V, Miyazaki K, Quaranta V. Role of cell surface metalloprotease MT1-MMP in epithelial cell migration over laminin-5. J Cell Biol 2000;148(3):615-624.
29. Holmbeck K, Bianco P, Pidoux I, Inoue S, Billinghurst RC, Wu W, Chrysovergis K, Yamada S, Birkedal-Hansen H, Poole AR. The metalloproteinase MT1-MMP is required for normal development and maintenance of osteocyte processes in bone. Journal of Cell Science 2005;118(1):147-156.
30. Knothe Tate ML. "Whither flows the fluid in bone?" An osteocyte's perspective. Journal of Biomechanics 2003;36(10):1409-1424.
31. Bustelo XR, Sauzeau V, Berenjeno IM. GTP-binding proteins of the Rho/Rac family: regulation, effectors and functions in vivo. BioEssays 2007;29(4):356-370.

32. Kamioka H, Honjo T, Takano-Yamamoto T. A three-dimensional distribution of osteocyte processes revealed by the combination of confocal laser scanning microscopy and differential interference contrast microscopy. Bone 2001;28(2):145-149.
33. Datta HK, Ng WF, Walker JA, Tuck SP, Varanasi SS. The cell biology of bone metabolism. Journal of Clinical Pathology 2008;61(5):577-587.
34. van Oers RFM, Ruimerman R, Tanck E, Hilbers PAJ, Huiskes R. A unified theory for osteonal and hemi-osteonal remodeling. Bone 2008;42(2):250-259.
35. Liu X-H, Kirschenbaum A, Weinstein BM, Zaidi M, Yao S, Levine AC. Prostaglandin E2 modulates components of the Wnt signaling system in bone and prostate cancer cells. Biochemical and Biophysical Research Communications 2010;394(3):715-720.
36. Tan SD, de Vries TJ, Kuijpers-Jagtman AM, Semeins CM, Everts V, Klein-Nulend J. Osteocytes subjected to fluid flow inhibit osteoclast formation and bone resorption. Bone 2007;41(5):745-751.
37. Bacabac RG, Mizuno D, Schmidt CF, MacKintosh FC, Van Loon JJWA, Klein-Nulend J, Smit TH. Round versus flat: Bone cell morphology, elasticity, and mechanosensing. Journal of Biomechanics 2008;41(7):1590-1598.
38. Tatsumi S, Ishii K, Amizuka N, Li M, Kobayashi T, Kohno K, Ito M, Takeshita S, Ikeda K. Targeted Ablation of Osteocytes Induces Osteoporosis with Defective Mechanotransduction. Cell Metabolism 2007;5(6):464-475.
39. Simonet WS, Lacey DL, Dunstan CR, Kelley M, Chang MS, Lüthy R, Nguyen HQ, Wooden S, Bennett L, Boone T and others. Osteoprotegerin: A Novel Secreted Protein Involved in the Regulation of Bone Density. Cell 1997;89(2):309-319.
40. Al-Dujaili SA, Lau E, Al-Dujaili H, Tsang K, Guenther A, You L. Apoptotic osteocytes regulate osteoclast precursor recruitment and differentiation in vitro. Journal of Cellular Biochemistry 2011;112(9):2412-2423.
41. Mann V, Huber C, Kogianni G, Jones D, Noble B. The influence of mechanical stimulation on osteocyte apoptosis and bone viability in human trabecular bone. J Musculoskelet Neuronal Interact 2006;6(4):408-417.
42. Gu G, Mulari M, Peng Z, Hentunen TA, Väänänen HK. Death of osteocytes turns off the inhibition of osteoclasts and triggers local bone resorption. Biochemical and Biophysical Research Communications 2005;335(4):1095-1101.
43. Kogianni G, Mann V, Noble BS. Apoptotic Bodies Convey Activity Capable of Initiating Osteoclastogenesis and Localized Bone Destruction. Journal of Bone and Mineral Research 2008;23(6):915-927.
44. McNamara LM, Majeska RJ, Weinbaum S, Friedrich V, Schaffler MB. Attachment of Osteocyte Cell Processes to the Bone Matrix. The Anatomical Record: Advances in Integrative Anatomy and Evolutionary Biology 2009;292(3):355-363.
45. Palumbo C, Palazzini S, Marotti G. Morphological study of intercellular junctions during osteocyte differentiation. Bone 1990;11(6):401-406.

46. Dallas SL, Bonewald LF. Dynamics of the transition from osteoblast to osteocyte. Annals of the New York Academy of Sciences 2010;1192(1):437-443.
47. Martín-Villar E, Scholl FG, Gamallo C, Yurrita MM, Muñoz-Guerra M, Cruces J, Quintanilla M. Characterization of human PA2.26 antigen (T1α–2, podoplanin), a small membrane mucin induced in oral squamous cell carcinomas. International Journal of Cancer 2005;113(6):899-910.
48. Negishi M, Katoh H. Rho Family GTPases and Dendrite Plasticity. The Neuroscientist 2005;11(3):187-191.
49. Pol A, Lu A, Pons Mn, PeirÃ³ S, Enrich C. Epidermal Growth Factor-mediated Caveolin Recruitment to Early Endosomes and MAPK Activation. Journal of Biological Chemistry 2000;275(39):30566-30572.
50. David M, Petit D, Bertoglio J. Cell cycle regulation of Rho signaling pathways. Cell Cycle 2012;11(16):0-7.
51. Penzes P, Jones KA. Dendritic spine dynamics - a key role for kalirin-7. Trends in Neurosciences 2008;31(8):419-427.
52. Rossman KL, Sondek J. Larger than Dbl: new structural insights into RhoA activation. Trends in Biochemical Sciences 2005;30(4):163-165.
53. Amano M, Fukata Y, Kaibuchi K. Regulation and Functions of Rho-Associated Kinase. Experimental Cell Research 2000;261(1):44-51.
54. Etienne-Manneville S, Hall A. Rho GTPases in cell biology. Nature 2002;420(6916):629-635.
55. Schmidt A, Hall A. Guanine nucleotide exchange factors for Rho GTPases: turning on the switch. Genes & Development 2002;16(13):1587-1609.
56. Rossman KL, Der CJ, Sondek J. GEF means go: turning on RHO GTPases with guanine nucleotide-exchange factors. Nat Rev Mol Cell Biol 2005;6(2):167-180.
57. Johnson RC, Penzes P, Eipper BA, Mains RE. Isoforms of Kalirin, a Neuronal Dbl Family Member, Generated through Use of Different 5'- and 3'-Ends Along with an Internal Translational Initiation Site. Journal of Biological Chemistry 2000;275(25):19324-19333.
58. Ma X, Huang J, Wang Y, Eipper B, Mains R. Kalirin, a multifunctional Rho guanine nucleotide exchange factor, is necessary for maintenance of hippocampal pyramidal neuron dendrites and dendritic spines. J Neurosci 2003;23(33):10593-10603.
59. Penzes P, Johnson RC, Sattler R, Zhang X, Huganir RL, Kambampati V, Mains RE, Eipper BA. The Neuronal Rho-GEF Kalirin-7 Interacts with PDZ Domain Containing Proteins and Regulates Dendritic Morphogenesis. Neuron 2001;29(1):229-242.
60. Muller D, Buchs P, Stoppini L. Time course of synaptic development in hippocampal organotypic cultures. Brain Res Dev Brain Res 1993;71(1):93-100.
61. Hansel DE, Quiñones ME, Ronnett GV, Eipper BA. Kalirin, a GDP/GTP Exchange Factor of the Dbl Family, Is Localized to Nerve, Muscle, and Endocrine Tissue During Embryonic Rat Development. Journal of Histochemistry & Cytochemistry 2001;49(7):833-844.

62. Mandela P, Ma X. Kalirin, a Key Player in Synapse Formation, Is Implicated in Human Diseases. Neural Plasticity 2012;2012:9.
63. Alam MR, Caldwell BD, Johnson RC, Darlington DN, Mains RE, Eipper BA. Novel Proteins That Interact with the COOH-terminal Cytosolic Routing Determinants of an Integral Membrane Peptide-processing Enzyme. Journal of Biological Chemistry 1996;271(45):28636-28640.
64. Ratovitski EA, Alam MR, Quick RA, McMillan A, Bao C, Kozlovsky C, Hand TA, Johnson RC, Mains RE, Eipper BA and others. Kalirin Inhibition of Inducible Nitric-oxide Synthase. Journal of Biological Chemistry 1999;274(2):993-999.
65. Colomer V, Engelender S, Sharp AH, Duan K, Cooper JK, Lanahan A, Lyford G, Worley P, Ross CA. Huntingtin-Associated Protein 1 (HAP1) Binds to a Trio-Like Polypeptide, with a rac1 Guanine Nucleotide Exchange Factor Domain. Human Molecular Genetics 1997;6(9):1519-1525.
66. Steven R, Kubiseski TJ, Zheng H, Kulkarni S, Mancillas J, Morales AR, Hogue CWV, Pawson T, Culotti J. UNC-73 Activates the Rac GTPase and Is Required for Cell and Growth Cone Migrations in C. elegans. Cell 1998;92(6):785-795.
67. Penzes P, Johnson RC, Kambampati V, Mains RE, Eipper BA. Distinct Roles for the Two Rho GDP/GTP Exchange Factor Domains of Kalirin in Regulation of Neurite Growth and Neuronal Morphology. The Journal of Neuroscience 2001;21(21):8426-8434.
68. Penzes P, Johnson RC, Sattler R, Zhang X, Huganir RL, Kambampati V, Mains RE, Eipper BA. The Neuronal Rho-GEF Kalirin-7 Interacts with PDZ Domain–Containing Proteins and Regulates Dendritic Morphogenesis. Neuron 2001;29(1):229-242.
69. Gorbatyuk V, Schiller M, Gorbatyuk O, Barwinski M, Hoch J. NMR structure note: N-terminal Dbl domain of the RhoGEF, Kalirin. J Biomol NMR 2012;52(3):269-276.
70. Xin X, Rabiner C, Mains R, Eipper B. Kalirin12 interacts with dynamin. BMC Neuroscience 2009;10(1):61.
71. Tskhovrebova L, Trinick J. Properties of Titin Immunoglobulin and Fibronectin-3 Domains. Journal of Biological Chemistry 2004;279(45):46351-46354.
72. Kontrogianni-Konstantopoulos A, Bloch RJ. The Hydrophilic Domain of Small Ankyrin-1 Interacts with the Two N-terminal Immunoglobulin Domains of Titin. Journal of Biological Chemistry 2003;278(6):3985-3991.
73. Schiller MR, Blangy A, Huang J, Mains RE, Eipper BA. Induction of lamellipodia by Kalirin does not require its guanine nucleotide exchange factor activity. Experimental Cell Research 2005;307(2):402-417.
74. Ma X-M, Wang Y, Ferraro F, Mains RE, Eipper BA. Kalirin-7 Is an Essential Component of both Shaft and Spine Excitatory Synapses in Hippocampal Interneurons. The Journal of Neuroscience 2008;28(3):711-724.
75. Huang S, Eleniste P, LeBlanc P, Brown D, Allen M, Bruzzaniti A. Kalirin Decreases Bone Mass Through Effects in Both Osteoclasts and Osteoblasts. 2012.

76. McPherson C, Eipper B, Mains R. Kalirin expression is regulated by multiple promoters. J Mol Neurosci 2004;22(1-2):51-62.
77. Stern A, Stern M, Van Dyke M, Jähn K, Prideaux M, Bonewald L. Isolation and culture of primary osteocytes from the long bones of skeletally mature and aged mice. Biotechniques 2012;52(6):361-373.
78. Qiu S, Fyhrie DP, Palnitkar S, Rao DS. Histomorphometric assessment of Haversian canal and osteocyte lacunae in different-sized osteons in human rib. The Anatomical Record Part A: Discoveries in Molecular, Cellular, and Evolutionary Biology 2003;272A(2):520-525.
79. Kato Y, Windle JJ, Koop BA, Mundy GR, Bonewald LF. Establishment of an Osteocyte-like Cell Line, MLO-Y4. Journal of Bone and Mineral Research 1997;12(12):2014-2023.
80. Ma X-M, Kiraly DD, Gaier ED, Wang Y, Kim E-J, Levine ES, Eipper BA, Mains RE. Kalirin-7 Is Required for Synaptic Structure and Function. The Journal of Neuroscience 2008;28(47):12368-12382.
81. Mains R, Kiraly D, Eipper-Mains J, Ma X-M, Eipper B. Kalrn promoter usage and isoform expression respond to chronic cocaine exposure. BMC Neuroscience 2011;12(1):20.
82. Bonewald LF, Johnson ML. Osteocytes, mechanosensing and Wnt signaling. Bone 2008;42(4):606-615.
83. Rosen CJ. Circulating IGF-I and bone remodeling: New insights into old questions. IBMS BoneKEy 2008;5(1):7-15.
84. Wang J, Zhou J, Bondy CA. Igf1 promotes longitudinal bone growth by insulin-like actions augmenting chondrocyte hypertrophy. The FASEB Journal 1999;13(14):1985-1990.
85. Pockwinse S, Wilming L, Conlon D, Stein G, Lian J. Expression of cell growth and bone specific genes at single cell resolution during development of bone tissue-like organization in primary osteoblast cultures. J Cell Biochem 1992;49(3):310-323.
86. Braidman IP, Davenport LK, Carter HD, Selby PL, Mawer BE, Freemont AJ. Preliminary in situ identification of estrogen target cells in bone. Journal of Bone and Mineral Research 1995;10(1):74-80.
87. Chakrabarti K, Lin R, Schiller NI, Wang Y, Koubi D, Fan Y-X, Rudkin BB, Johnson GR, Schiller MR. Critical Role for Kalirin in Nerve Growth Factor Signaling through TrkA. Molecular and Cellular Biology 2005;25(12):5106-5118.
88. Kim SY, Shin DH, Kim SJ, Koo B-S, Bae C-D, Park J, Jeon S. Chloride channel conductance is required for NGF-induced neurite outgrowth in PC12 cells. Neurochemistry International 2010;56(5):663-669.
89. Brand F, Schumacher S, Kant S, Menon MB, Simon R, Turgeon B, Britsch S, Meloche S, Gaestel M, Kotlyarov A. The Extracellular Signal-Regulated Kinase 3 (Mitogen-Activated Protein Kinase 6 [MAPK6])–MAPK-Activated Protein Kinase 5 Signaling Complex Regulates Septin Function and Dendrite Morphology. Molecular and Cellular Biology 2012;32(13):2467-2478.

90. Christenson RH. Biochemical Markers of Bone Metabolism: An Overview. Clinical Biochemistry 1997;30(8):573-593.
91. Baron R, Rawadi G. Targeting the Wnt/beta-Catenin Pathway to Regulate Bone Formation in the Adult Skeleton. Endocrinology 2007;148(6):2635-2643.
92. Eriksen EF, Charles P, Melsen F, Mosekilde L, Risteli L, Risteli J. Serum markers of type I collagen formation and degradation in metabolic bone disease: Correlation with bone histomorphometry. Journal of Bone and Mineral Research 1993;8(2):127-132.
93. Gaur T, Lengner CJ, Hovhannisyan H, Bhat RA, Bodine PVN, Komm BS, Javed A, van Wijnen AJ, Stein JL, Stein GS and others. Canonical WNT Signaling Promotes Osteogenesis by Directly Stimulating Runx2 Gene Expression. Journal of Biological Chemistry 2005;280(39):33132-33140.
94. Igwe J, Gao Q, Kizivat T, Kao W, Kalajzic I. Keratocan is Expressed by Osteoblasts and Can Modulate Osteogenic Differentiation. Connective Tissue Research 2011;52(5):401-407.
95. Kanbur N, Derman O, Sen T, Kinik E. Osteocalcin. A biochemical marker of bone turnover during puberty. Int J Adolesc Med Health 2002;14(3):235-244.
96. Reinholt FP, Hultenby K, Oldberg A, HeinegÃ¥rd D. Osteopontin--a possible anchor of osteoclasts to bone. Proceedings of the National Academy of Sciences 1990;87(12):4473-4475.
97. Teitelbaum S. Osteoclasts: what do they do and how do they do it? Am J Pathol. 2007;170(2):427-435.
98. Nakashima K, Zhou X, Kunkel G, Zhang Z, Deng JM, Behringer RR, de Crombrugghe B. The Novel Zinc Finger-Containing Transcription Factor Osterix Is Required for Osteoblast Differentiation and Bone Formation. Cell 2002;108(1):17-29.
99. Fisher LW, Fedarko NS. Six Genes Expressed in Bones and Teeth Encode the Current Members of the SIBLING Family of Proteins. Connective Tissue Research 2003;44:33-40.
100. Zhang K, Barragan-Adjemian C, Ye L, Kotha S, Dallas M, Lu Y, Zhao S, Harris M, Harris S, Feng J and others. E11/gp38 selective expression in osteocytes: regulation by mechanical strain and role in dendrite elongation. Mol Cell Biol 2006;26(12):4539-4552.
101. Karadag A, Fedarko NS, Fisher LW. Dentin Matrix Protein 1 Enhances Invasion Potential of Colon Cancer Cells by Bridging Matrix Metalloproteinase-9 to Integrins and CD44. Cancer Research 2005;65(24):11545-11552.
102. Bonewald LF. The amazing osteocyte. Journal of Bone and Mineral Research 2011;26(2):229-238.
103. Lu Y, Yuan B, Qin C, Cao Z, Xie Y, Dallas SL, McKee MD, Drezner MK, Bonewald LF, Feng JQ. The biological function of DMP-1 in osteocyte maturation is mediated by its 57-kDa c-terminal fragment. Journal of Bone and Mineral Research 2011;26(2):331-340.
104. Hasegawa T, Amizuka N, Yamada T, Liu Z, Miyamoto Y, Yamamoto T, Sasaki M, Hongo H, Suzuki R, De Freitas PHL and others. Sclerostin is differently immunolocalized in metaphyseal trabecules and cortical bones of mouse tibiae. Biomedical Research 2013;34(3):153-159.

105. Toyosawa S, Shintani S, Fujiwara T, Ooshima T, Sato A, Ijuhin N, Komori T. Dentin Matrix Protein 1 Is Predominantly Expressed in Chicken and Rat Osteocytes But Not in Osteoblasts. Journal of Bone and Mineral Research 2001;16(11):2017-2026.
106. Kalajzic I, Braut A, Guo D, Jiang X, Kronenberg MS, Mina M, Harris MA, Harris SE, Rowe DW. Dentin matrix protein 1 expression during osteoblastic differentiation, generation of an osteocyte GFP-transgene. Bone 2004;35(1):74-82.
107. Lee K, Jessop H, Suswillo R, Zaman G, Lanyon L. The adaptive response of bone to mechanical loading in female transgenic mice is deficient in the absence of oestrogen receptor-alpha and -beta. Journal of Endocrinology 2004;182(2):193-201.
108. Liu S, Zhou J, Tang W, Jiang X, Rowe DW, Quarles LD. Pathogenic role of Fgf23 in Hyp mice. American Journal of Physiology - Endocrinology And Metabolism 2006;291(1):E38-E49.
109. Liu S, Tang W, Fang J, Ren J, Li H, Xiao Z, Quarles LD. Novel Regulators of Fgf23 Expression and Mineralization in Hyp Bone. Molecular Endocrinology 2009;23(9):1505-1518.
110. Feng JQ, Ward LM, Liu S, Lu Y, Xie Y, Yuan B, Yu X, Rauch F, Davis SI, Zhang S and others. Loss of DMP1 causes rickets and osteomalacia and identifies a role for osteocytes in mineral metabolism. Nat Genet 2006;38(11):1310-1315.
111. Nampei A, Hashimoto J, Hayashida K, Tsuboi H, Shi K, Tsuji I, Miyashita H, Yamada T, Matsukawa N, Matsumoto M and others. Matrix extracellular phosphoglycoprotein (MEPE) is highly expressed in osteocytes in human bone. Journal of Bone and Mineral Metabolism 2004;22(3):176-184.
112. Kulkarni R, Bakker A, Everts V, Klein-Nulend J. Inhibition of Osteoclastogenesis by Mechanically Loaded Osteocytes: Involvement of MEPE. Calcified Tissue International 2010;87(5):461-468.
113. Rowe PSN, Kumagai Y, Gutierrez G, Garrett IR, Blacher R, Rosen D, Cundy J, Navvab S, Chen D, Drezner MK and others. MEPE has the properties of an osteoblastic phosphatonin and minhibin. Bone 2004;34(2):303-319.
114. Atkins GJ, Rowe PS, Lim HP, Welldon KJ, Ormsby R, Wijenayaka AR, Zelenchuk L, Evdokiou A, Findlay DM. Sclerostin is a locally acting regulator of late-osteoblast/preosteocyte differentiation and regulates mineralization through a MEPE-ASARM-dependent mechanism. Journal of Bone and Mineral Research 2011;26(7):1425-1436.
115. Pockwinse S, Wilming L, Conlon D, Stein G, Lian J. Expression of cell growth and bone specific genes at single cell resolution during development of bone tissue-like organization in primary osteoblast cultures. J Cell Biochem Suppl 1992;49(3):310-323.
116. Lin C, Jiang X, Dai Z, Guo X, Weng T, Wang J, Li Y, Feng G, Gao X, He L. Sclerostin Mediates Bone Response to Mechanical Unloading Through Antagonizing Wnt/β-Catenin Signaling. Journal of Bone and Mineral Research 2009;24(10):1651-1661.
117. Winkler DG, Sutherland MK, Geoghegan JC, Yu C, Hayes T, Skonier JE, Shpektor D, Jonas M, Kovacevich BR, Staehling-Hampton K and others. Osteocyte control of bone formation via sclerostin, a novel BMP antagonist. EMBO J 2003;22(23):6267-6276.

118. Wesseling-Perry K. FGF-23 in bone biology. Pediatric Nephrology 2010;25(4):603-608.
119. Feng J, Ward L, Liu S, Lu Y, Xie Y, Yuan B, Yu X, Rauch F, Davis S, Zhang S and others. Loss of DMP1 causes rickets and osteomalacia and identifies a role for osteocytes in mineral metabolism. Nat Genet 2006;38(11):1310-1315.
120. Bord S, Horner A, Beavan S, Compston J. Estrogen Receptors α and β Are Differentially Expressed in Developing Human Bone. Journal of Clinical Endocrinology & Metabolism 2001;86(5):2309-2314.
121. Nilsson LO, Boman A, Sävendahl L, Grigelioniene G, Ohlsson C, Ritzén EM, Wroblewski J. Demonstration of Estrogen Receptor-β Immunoreactivity in Human Growth Plate Cartilage. Journal of Clinical Endocrinology & Metabolism 1999;84(1):370-373.
122. McPherson CE, Eipper BA, Mains RE. Genomic organization and differential expression of Kalirin isoforms. Gene 2002;284(1–2):41-51.
123. Phimphilai M, Zhao Z, Boules H, Roca H, Franceschi RT. BMP Signaling Is Required for RUNX2-Dependent Induction of the Osteoblast Phenotype. Journal of Bone and Mineral Research 2006;21(4):637-646.
124. Zhang C. Molecular mechanisms of osteoblast-specific transcription factor Osterix effect on bone formation. Beijing Da Xue Xue Bao 2012;44(5):659-665.
125. Devescovi V, Leonardi E, Ciapetti G, Cenni E. Growth factors in bone repair. La Chirurgia degli Organi di Movimento 2008;92(3):161-168.
126. Cheng S-L, Shao J-S, Charlton-Kachigian N, Loewy AP, Towler DA. Msx2 Promotes Osteogenesis and Suppresses Adipogenic Differentiation of Multipotent Mesenchymal Progenitors. Journal of Biological Chemistry 2003;278(46):45969-45977.
127. Bikle D, Wang Y. Insulin like growth factor-I: a critical mediator of the skeletal response to parathyroid hormone. Curr Mol Pharmacol 2012;5(2):135-142.
128. Bellows CG, Ishida H, Aubin JE, Heersche JNM. Parathyroid Hormone Reversibly Suppresses the Differentiation of Osteoprogenitor Cells into Functional Osteoblasts. Endocrinology 1990;127(6):3111-3116.
129. Feng JQ, Huang H, Lu Y, Ye L, Xie Y, Tsutsui TW, Kunieda T, Castranio T, Scott G, Bonewald LB and others. The Dentin Matrix Protein 1 (Dmp1) is Specifically Expressed in Mineralized, but not Soft, Tissues during Development. Journal of Dental Research 2003;82(10):776-780.
130. Qin C, Baba O, Butler WT. Post-translational Modifications of SIBLING Proteins and Their Roles in Osteogenesis and Dentinogenesis. Critical Reviews in Oral Biology & Medicine 2004;15(3):126-136.
131. Gowen LC, Petersen DN, Mansolf AL, Qi H, Stock JL, Tkalcevic GT, Simmons HA, Crawford DT, Chidsey-Frink KL, Ke HZ and others. Targeted Disruption of the Osteoblast/Osteocyte Factor 45 Gene (OF45) Results in Increased Bone Formation and Bone Mass. Journal of Biological Chemistry 2003;278(3):1998-2007.

132. Rowe PSN. The Wrickkened Pathways of FGF23, MEPE and PHEX. Critical Reviews in Oral Biology & Medicine 2004;15(5):264-281.
133. Pederson L, Ruan M, Westendorf JJ, Khosla S, Oursler MJ. Regulation of bone formation by osteoclasts involves Wnt/BMP signaling and the chemokine sphingosine-1-phosphate. Proceedings of the National Academy of Sciences 2008;105(52):20764-20769.
134. Bennett CN, Longo KA, Wright WS, Suva LJ, Lane TF, Hankenson KD, MacDougald OA. Regulation of osteoblastogenesis and bone mass by Wnt10b. Proceedings of the National Academy of Sciences of the United States of America 2005;102(9):3324-3329.
135. Sims NA. EPHs and ephrins: Many pathways to regulate osteoblasts and osteoclasts. IBMS BoneKEy 2010;7(9):304-313.
136. Kramer I, Halleux C, Keller H, Pegurri M, Gooi JH, Weber PB, Feng JQ, Bonewald LF, Kneissel M. Osteocyte Wnt/β-Catenin Signaling Is Required for Normal Bone Homeostasis. Molecular and Cellular Biology 2010;30(12):3071-3085.
137. Schaffler M, Kennedy O. Osteocyte Signaling in Bone. Current Osteoporosis Reports 2012;10(2):118-125.
138. Beno T, Yoon Y-J, Cowin SC, Fritton SP. Estimation of bone permeability using accurate microstructural measurements. Journal of Biomechanics 2006;39(13):2378-2387.
139. Bonewald LF. Osteocytes as Dynamic Multifunctional Cells. Annals of the New York Academy of Sciences 2007;1116(1):281-290.
140. Li X, Zhang Y, Kang H, Liu W, Liu P, Zhang J, Harris SE, Wu D. Sclerostin Binds to LRP5/6 and Antagonizes Canonical Wnt Signaling. Journal of Biological Chemistry 2005;280(20):19883-19887.
141. Veverka V, Henry AJ, Slocombe PM, Ventom A, Mulloy B, Muskett FW, Muzylak M, Greenslade K, Moore A, Zhang L and others. Characterization of the Structural Features and Interactions of Sclerostin: molecular insight into a key regulator of Wnt-mediated bone formation. Journal of Biological Chemistry 2009;284(16):10890-10900.
142. Kumar V, Green S, Staub A, Chambon P. Localisation of the oestradiol-binding and putative DNA-binding domains of the human oestrogen receptor. EMBO J 1986;5(9):2231-2236.
143. Nakamura T, Imai Y, Matsumoto T, Sato S, Takeuchi K, Igarashi K, Harada Y, Azuma Y, Krust A, Yamamoto Y and others. Estrogen Prevents Bone Loss via Estrogen Receptor ± and Induction of Fas Ligand in Osteoclasts. Cell 2007;130(5):811-823.
144. Courtland H-W, Sun H, Beth-On M, Wu Y, Elis S, Rosen CJ, Yakar S. Growth hormone mediates pubertal skeletal development independent of hepatic IGF-1 production. Journal of Bone and Mineral Research 2011;26(4):761-768.
145. Lean J, Mackay A, Chow J, Chambers T. Osteocytic expression of mRNA for c-fos and IGF-I: an immediate early gene response to an osteogenic stimulus. Am J Physiol 1996;6(1):937-945.
146. Zhao G, Monier-Faugere M-C, Langub MC, Geng Z, Nakayama T, Pike JW, Chernausek SD, Rosen CJ, Donahue L-R, Malluche HH and others. Targeted Overexpression of Insulin-Like

Growth Factor I to Osteoblasts of Transgenic Mice: Increased Trabecular Bone Volume without Increased Osteoblast Proliferation. Endocrinology 2000;141(7):2674-2682.

147. Plotkin LI, Mathov I, Aguirre JI, Parfitt AM, Manolagas SC, Bellido T. Mechanical stimulation prevents osteocyte apoptosis: requirement of integrins, Src kinases, and ERKs. American Journal of Physiology - Cell Physiology 2005;289(3):C633-C643.
148. Plotkin LI, Aguirre JI, Kousteni S, Manolagas SC, Bellido T. Bisphosphonates and Estrogens Inhibit Osteocyte Apoptosis via Distinct Molecular Mechanisms Downstream of Extracellular Signal-regulated Kinase Activation. Journal of Biological Chemistry 2005;280(8):7317-7325.

ABSTRACT

KALIRIN: NOVEL ROLE IN OSTEOCYTE FUNCTION

K. Wayakanon*, S. Huang, P. Eleniste, M. Allen and A. Bruzzaniti

Indiana University School of Dentistry, Indianapolis, IN

Communication between bone cells is important for the maintenance of bone mass. Although osteocytes are deeply embedded within the mineralized matrix, they are essential for the regulation of osteoblast and osteoclast functions. However, the intracellular proteins that control the morphology and function of osteocytes, and their ability to communicate with other bone cells are still unknown. Kalirin is a novel multi-domain GTP exchange factor (GEF) protein that activates the RhoGTPases. Recently, we found that 14 week old female Kalirin knockout (Kal-KO) mice exhibit a 45% decrease in trabecular bone density and have significantly lower cortical area, perimeter, thickness and polar cross-sectional moment of inertia (-12.6%, -7.2%, -7.6% and -21.9%, respectively) than WT mice. Kalirin was found to be expressed in osteoclasts and osteoblasts but its expression and function in osteocytes is currently unclear. We examined the role of Kalirin on the morphology and function of osteocytes. Primary osteocytes were isolated by sequential collagenase digestions from long bones (femurs and tibias) of 10-week old WT and Kal-KO mice. Immunofluorescent staining revealed Kalirin was localized to the perinuclear region of primary osteocytes and MLO-Y4 cells, and was detected along the cytoplasmic processes of primary osteocytes. We also examined primary osteocytes isolated from the long bones of Kal-KO and WT mice for changes in the length and number of cytoplasmic processes. Kal-KO osteocytes were found to express significantly fewer cytoplasmic processes per cell (3.3±0.21) than WT osteocytes (4.7±0.3). In addition, the cytoplasmic processes of Kal-KO osteocytes were shorter (79.5±4.6 μm) than those observed for WT osteocytes (85.4±3.6 μm) (p <0.01). Quantitative PCR revealed the expression of mRNA for the three major Kalirin isoforms (Kal-7, Kal-9, Kal-12) in primary osteocytes and in MLO-Y4 cells. Moreover, the mRNA levels of osteoprotegerin (OPG) and SOST, which are important for controlling osteoclast differentiation and Wnt signaling leading to bone formation, respectively, were reduced in Kal-KO osteocytes. Next, the role of Kalirin in osteocyte morphology and function was further examined. Treatment of MLO-Y4 cells for 5 days with nerve growth factor, which is known to activate Kalirin in neurons, or over-expression of the Ser-Thr kinase domain of Kal-12, promoted cytoplasmic process elongation and upregulated phosphorylated ERK and RhoA levels. Together, these results suggest that Kalirin controls osteocyte morphology and function in part by regulating cytoskeletal remodeling and the activity of ERK and RhoA. Furthermore, Kalirin may control the bone remodeling cycle by regulating osteocyte signaling to osteoclasts and osteoblasts.

CURRICULUM VITAE

Kornchanok Wayakanon, DDS., Ph.D.

1997-2003	Chulalongkorn University, Bangkok, Thailand Degree: Doctor of Dental Surgery (DDS.) Research project: Comparison between Penetrating Abilities of Sealant and Depth of Pits and Fissures
2007-2011	Department of Oral and Maxillofacial Surgery, School of Clinical Dentistry, University of Sheffield, Sheffield, United Kingdom Degree: Doctor of Philosophy (Ph.D.) Research project: Intracellular antibiotic therapy using polymer nano-vesicles for *Porphyromonas gingivalis* infected keratinocytes
2011-present	Department of Restorative Dentistry, School of Dentistry, Indiana University, Indianapolis, Indiana, USA Degree: Master of Science in Dentistry (MSD) Research project: Kalirin: Novel Role in Osteocyte Function

Professional and Scientific experience:

- 2000: Clinical research project championship award, Chulalongkorn University, Thailand
- 2003-present: Full-time faculty member, Department of Restorative Dentistry, Faculty of Dentistry, Naresuan University, Thailand
- 2008: Awarded grant "Oral and Dental Research Trust", United Kingdom
- 2009: Oral competition in British Society Dental Research (BSDR), Glasgow, United Kingdom
- 2010: Oral presentation in International Association for Dental Research (IADR), Barcelona, Spain
- 2010: Oral presentation in International Association of Science and Technology for Development (IASTED), Cambridge, Massachusetts, USA
- 2010: Awarded 2nd place Medicine category , Anglo Thai Society, London, United Kingdom
- 2013: Poster presentation in International Association for Dental Research (IADR), Seattle, Washington, USA
- 2013: Poster competition in Research day, Indiana section of the AADR (INAADR), Indiana University School of Dentistry, Indiana, USA
- 2013: Awarded Delta Dental Award for Innovation in Oral Care Research, Indiana University School of Dentistry, Indiana, USA
- 2013: President's Poster Award Competition in the American Society for Bone and Mineral Research (ASBMR) in Baltimore, Maryland, USA